Nonperturbatively determined relativistic heavy quark action

Huey-Wen Lin* and Norman Christ†

Physics Department, Columbia University, New York, New York 10027, USA

(Received 9 October 2006; published 29 October 2007)

We present a method to nonperturbatively determine the parameters of the on-shell, $O(a)$-improved relativistic heavy quark action. These three parameters, m_0, ζ, and $c_B = c_E$, are obtained by matching finite-volume, heavy-heavy, and heavy-light meson masses to the exact relativistic spectrum through a finite-volume, step-scaling recursion procedure. We demonstrate that accuracy on the level of a few percent can be achieved by carrying out this matching on a pair of lattices with equal physical spatial volumes but quite different lattice spacings. A fine lattice with inverse lattice spacing $1/a = 5.4$ GeV and $24^3 \times 48$ sites and a coarse, $1/a = 3.6$ GeV, $16^3 \times 32$ lattice are used together with a heavy quark mass m approximately that of the charm quark. This approach is unable to determine the initially expected, four heavy quark parameters: m_0, ζ, c_B, and c_E. This apparent nonuniqueness of these four parameters motivated the analytic result, presented in a companion paper, that this set is redundant and that the restriction $c_E = c_B$ is permitted through order $a|\vec{p}|$ and to all orders in ma where $\vec{p}$ is the heavy quark's spatial momenta.

DOI: 10.1103/PhysRevD.76.074506 PACS numbers: 11.15.Ha, 12.38.Gc, 12.38.Lg, 14.40.−n

I. INTRODUCTION

The study of flavor physics and CP violation plays a central role in particle physics. In particular, many of the parameters of the standard model can be constrained by measurements of the properties of hadrons containing heavy quarks. However, to do this one needs theoretical determination of strong-interaction masses and matrix elements to connect the experimental measurements with those fundamental quantities. Lattice quantum chromodynamics (QCD) provides a first-principles method for the computation of these hadronic masses and matrix elements. However, lattice calculations with heavy quarks present special difficulties since in full QCD calculations, which properly include the effects of dynamical quarks, it is impractical to work with lattice spacings sufficiently small that errors on the order of ma can be controlled. These problems are addressed by using a number of improved heavy quark actions designed to control or avoid these potentially important finite lattice spacing errors. The results of recent calculations of basic parameters of the standard model can be found in the lattice heavy quark reviews of Refs. [1–5].

A variety of fermion actions have been used in lattice calculations involving heavy quarks. These include heavy quark effective theory [6] (HQET) (for which the static approximation is the leading term) and nonrelativistic QCD [7] (NRQCD). These methods have significant limitations: NRQCD has no continuum limit, and although HQET has a continuum limit, it cannot be applied to quarkonia. While systems involving bottom quarks may permit a successful expansion in inverse powers of m, this is likely not true for systems including a charm quark.

A third approach, the one adopted here, is the Fermilab or relativistic heavy quark (RHQ) method [8,9] in which extra axis-interchange asymmetric terms are added to the usual relativistic action. As is discussed below, this action can accurately describe heavy quark systems provided the improvement coefficients it contains are properly adjusted. As the heavy quark mass decreases, this action goes over smoothly to the order a improved fermion action of Sheikholeslami and Wohlert (SW) [10]. Thus, it seems appropriate to refer to this as the relativistic heavy quark method since it retains the relativistic form of the Wilson fermion action (with the exception that lattice axis-interchange symmetry is broken) and approaches the standard relativistic action as ma becomes small.

As is discussed in the original papers [8,9] and considered in detail in our companion paper [11], this approach builds upon the original work of Sheikholeslami and Wohlert, extending it to the case of a possibly very heavy quark with mass $m \geq 1/a$ but restricted to a reference system in which these quarks are nearly at rest. Such a situation can be described by a Symanzik effective Lagrangian [12] which contains terms of higher dimension than four which explicitly reproduce the finite lattice spacing errors implied by the lattice Lagrangian.

In this RHQ approach, the continuum effective Lagrangian is imagined to reproduce errors of first order in $a|\vec{p}|$ and all orders in ma or $p_0 a$, where $(\vec{p}, p^0)$ is the heavy quark four-momentum. Such an effective action will contain many terms, including those with arbitrarily large powers of the combination aD^0 where the gauge-covariant time derivative D^0 will introduce a factor of p^0 and so cannot be neglected. As described in Ref. [8] and discussed in detail in our companion paper, this Lagrangian can be greatly simplified by performing field transformations within the path integral for the effective theory. These field transformations do not change the particle masses pre-

*hwlin@phys.columbia.edu
†nhc@phys.columbia.edu

dicted by the theory and, as is discussed in Ref. [11], they effect on-shell spinor Green's functions only by a simple, Lorentz noncovariant, 4×4 spinor rotation. (The use of the equations of motion in Ref. [9] is equivalent to the above field transformation approach.)

As is shown in our companion paper [11], after this simplification, the resulting effective Lagrangian contains only three parameters: the quark mass m^c, an asymmetry parameter ζ^c describing the ratio of the coefficients of the spatial and temporal derivative, and a generalization of the Sheikholeslami and Wohlert c_{SW} to the case of nonzero mass which we refer to as c_P^c. Here the superscript c indicates that these are the coefficients that appear in the continuum effective Lagrangian. If these three, mass-dependent parameters can be tuned to physical continuum values (m^c, 1 and 0, respectively) by the proper choice of mass-dependent coefficients in the lattice action, then the hadronic masses computed in the resulting theory will contain errors no larger than $(\vec{p}a)^2$.

It is important to recognize that such order $(\vec{p}a)^2$ terms will have coefficients which are not simple constants but actual functions of the variable ma. Thus, in order to neglect such terms, we must assume that their coefficients remain bounded as ma varies over the relevant range. That this assumption is obeyed can be checked at tree level and may be true more generally because the heavy quark propagator is a decreasing function of the heavy quark mass [8].

In addition, a new parameter δ multiplying a noncovariant $\vec{\gamma} \cdot \vec{p}$ in the 4×4 spinor matrix mentioned above will be needed to realize truly covariant on-shell Greens functions. Here δ will depend on the (usually composite) fermion operator being used even for a fixed action. As is discussed below and in detail in Ref. [11], this is one fewer parameter than found in the previous work of the Fermilab and Tsukuba groups.

Thus, in our calculation we use the relativistic heavy quark lattice action:

$$S_{\mathrm{lat}} = \sum_{n',n} \bar{\psi}_{n'} \Big(\gamma_0 D_0 + \zeta \vec{\gamma} \cdot \vec{D} + m_0 a - \frac{1}{2} r_t D_0^2 - \frac{1}{2} r_s \vec{D}^2 + \sum_{i,j} \frac{i}{4} c_B \sigma_{ij} F_{ij} + \sum_i \frac{i}{2} c_E \sigma_{0i} F_{0i} \Big)_{n',n} \psi_n, \tag{1}$$

where

$$D_\mu \psi(x) = \tfrac{1}{2}[U_\mu(x)\psi(x+\hat{\mu}) - U_\mu^\dagger(x-\hat{\mu})\psi(x-\hat{\mu})] \tag{2}$$

$$D_\mu^2 \psi(x) = [U_\mu(x)\psi(x+\hat{\mu}) + U_\mu^\dagger(x-\hat{\mu})\psi(x-\hat{\mu}) - 2\psi(x)] \tag{3}$$

$$F_{\mu\nu}\psi(x) = \frac{1}{8} \sum_{s,s'=\pm 1} s s' [U_{s\mu}(x) U_{s'\nu}(x + s\hat{\mu}) \times U_{-s\mu}(x + s\hat{\mu} + s'\hat{\nu}) \times U_{-s'\nu}(x + s'\hat{\nu}) - \mathrm{H.c.}]\psi(x) \tag{4}$$

and the γ matrices satisfy $\gamma_\mu = \gamma_\mu^\dagger, \{\gamma_\mu, \gamma_\nu\} = 2\delta_{\mu\nu}$, and $\sigma_{\mu\nu} = \frac{i}{2}[\gamma^\mu, \gamma^\nu]$. Written in this standard form, there are six possible parameters that can be adjusted to improve the resulting long-distance theory, three more than are needed. We begin by making the choice $r_s = \zeta$ and $r_t = 1$. This leaves four parameters whose effects we can study. In the following we will investigate the nonperturbative effects of these four parameters, $m_0 a$, ζ, c_B, and c_E. However, when determining an improved RHQ action nonperturbatively, we will impose the further restriction $c_B = c_E$, making the improved action uniquely defined at our order of approximation.

The different coefficient choices of improved lattice action by the Fermilab and Tsukuba groups yield two distinct sets of coefficients for the action. These are summarized in Table I. The coefficients in each approach have been calculated by applying lattice perturbation theory at the $O(a)$-improved, one-loop level to the quark propagator and quark-quark scattering amplitude [13,14].

In this paper, we will propose and demonstrate a nonperturbative method for determining these coefficients based on a step-scaling approach, which eliminates all errors of $O(g^{2n})$. Step-scaling has been used in the past to connect the lattice spacing accessible in large-volume simulations with a lattice scale sufficiently small that perturbation theory becomes accurate [15,16]. Nonperturbative matching conditions are imposed to connect the original calculation with one performed at a smaller lattice spacing $a_1' = a\epsilon$. Iterative matching of this sort with n steps then connects the theory of interest and a target lattice theory defined with lattice spacing $a_n' = a\epsilon^n$. This may require a number of steps n which is not too large since, while the coupling constant decreases only logarithmically with the energy scale, that energy scale increases exponentially with n. For example, if a final comparison with order g^2 perturbation theory is used, we

TABLE I. Comparison of the conventions and/or values used to specify the six terms in the improved lattice action of Eq. (1). The top row identifies terms that appear in Eq. (1). The next row lists our choice for the coefficient of each term and the next two rows specify that same coefficient written in the notation of the Fermilab [8] and Tsukuba [9] papers.

Action	$\gamma^0 D^0$	$\vec{\gamma}\vec{D}$	$-D_0^2$	$-(\vec{D})^2$	$\frac{i}{2}\sigma_{ij}F_{ij}$	$i\sigma_{0i}F_{0i}$
This paper	1	ζ	1	r_s	c_B	c_E
Fermilab	1	ζ	1	$r_s\zeta$	$c_B\zeta$	$c_E\zeta$
Tsukuba	1	ν	1	r_s	c_B	c_E

expect an error of order $(g')^4 \sim \ln(a'_n)^{-2} \sim n^{-2}$, where g' is the bare coupling for the finest lattice.

The situation for heavy quarks is even more favorable. Here the target, comparison theory does not need to have such small lattice spacing that perturbation theory is accurate. In fact, this theory can be treated nonperturbatively provided the final lattice spacing a'_n is sufficiently small that simulations with an ordinary $O(a)$-improved relativistic action will give accurate results [17]. This implies that the size of the error will be of order $(ma')^2 \sim n^{-2}$ or $n \sim (\text{error})^{-1/2}$. In the work reported here we will match the step-scaled heavy quark theory with an $O(a)$-accurate lattice calculation performed using domain wall fermions.

A critical question in developing such a step-scaling approach is to decide upon the actual quantities that will be ''matched'' when comparing two theories defined with different lattice spacings but which are intended to be physically equivalent. Among the quantities which might be matched are the Schrödinger functional [18–20], off-shell Green's functions defined in the RI/MOM scheme [21] or physical masses, and matrix elements at finite volume.

Our first approach to this topic was to investigate the off-shell RI/MOM scheme since this method had worked well in earlier light quark calculations, see e.g. Refs. [22,23], and also permits a direct comparison with quantities defined in perturbation theory. We were able to define RI/MOM kinematics which lay within the regime of validity of the effective heavy quark theory described above and to carry out a tree-level calculation of the amplitudes of interest [24,25]. However, the increased number of parameters needed in the effective theory to describe off-shell amplitudes, the need to work with gauge-noninvariant quantities, and the difficulty of computing ''disconnected'' gluon correlation functions ultimately made this approach appear impractical.

In this paper, we adopt the third method mentioned above and determine the coefficients in the heavy quark effective action appearing in our step-scaling procedure by requiring that the physical, momentum-dependent mass spectrum of two physically equivalent theories agree when compared on the same physical volume. Since the step-scaling approach requires physically small volumes be studied, these spectra will be significantly distorted by the effects of finite volume and it is important that these effects be the same in each of the theories being compared—thus the need to compare on identical physical volumes. By comparing more physical, finite-volume quantities (as many as seven) than there are parameters to adjust (three), we also have an overall consistency test of the method. Finally, as described above, at the smallest lattice spacing, we compute the quantities being compared using a standard domain wall fermion (DWF) action which has no order ma errors and accurate chiral symmetry. We assume that at this smallest lattice spacing the explicit errors of order $(ma)^2$, present in the domain wall fermion calculation, are sufficiently small to be neglected. Preliminary results using this method were published in Ref. [26].

The structure of this paper is as follows. We introduce our on-shell approach to determine the coefficients in the relativistic heavy quark action via step-scaling both in the quenched approximation and for full QCD in Sec. II. In this paper we will work in the quenched approximation and explicitly carry out the first stage of matching between a fine and a coarse lattice in order to determine the feasibility of this approach and the accuracy that can be achieved. Specifically the ''fine'' lattice uses $1/a = 5.4$ GeV and the ''coarse'' lattice $1/a = 3.6$ GeV. (A second matching step, evaluating the first coarse-lattice action on a larger physical volume and matching to an even larger lattice spacing, $1/a = 2.4$ GeV, is now underway [27].) Section III lists the parameters used in this calculation, describes our determination of the lattice spacing, and discusses our method for obtaining the physical heavy-heavy and heavy-light spectrum.

The problem of determining the parameters to be used in the coarse-lattice action which will reproduce the fine-lattice mass spectrum is studied in Sec. IV and the dependence of this spectrum on the four parameters $m_0 a$, ζ, c_B, and c_E presented. We are unable to determine these four parameters with any reasonable precision, a conclusion we now understand since only three parameters are required to determine the mass spectrum to order $a|\vec{p}|$ and all orders in $(ma)^n$ [11]. We then restrict the parameter space to $c_B = c_E$, as is justified theoretically, and find that the resulting three parameters can now be determined quite accurately. In Sec. V we compare our result with both perturbative and nonperturbative determinations of the quark mass and the one-loop lattice perturbation calculation of the lattice parameters ζ, c_B and c_E performed by Nobes [28]. Section VI presents a summary and outlook for this approach.

II. STRATEGY

We propose to determine the three coefficients $m_0 a$, ζ, and $c_P \equiv c_B = c_E$ in the RHQ lattice action of Eq. (1) by carrying out a series of matching steps. We begin with a sufficiently fine lattice spacing that no heavy quark improvements are needed ($ma \ll 1$) and a conventional light quark calculation will give accurate results. We then carry out a series of calculations using the RHQ lattice action of Eq. (1) on lattices with increasingly large lattice spacing and increasingly large physical volume. When we increase the lattice spacing at fixed physical volume, we perform calculations at both lattice spacings on identical physical volumes and require that the resulting finite-volume, heavy-heavy, and heavy-light energy spectra agree when these particles are at rest or have small spatial momenta. When we increase the lattice volume at fixed lattice spacing, we simply use the parameters, previously determined,

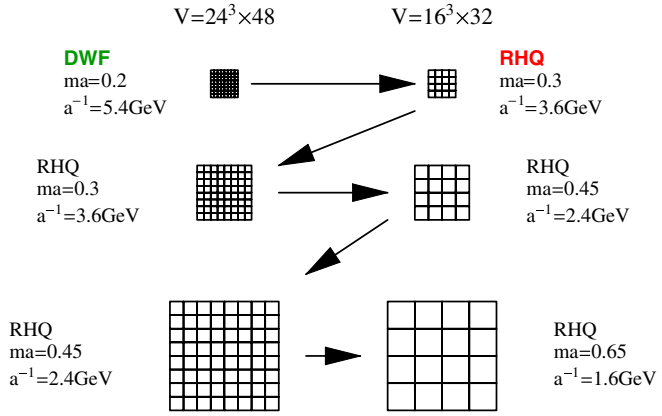

FIG. 1 (color online). The sequence of lattice sizes and lattice spacings used to determine the coarse-lattice, heavy quark parameters through a step-scaling technique beginning with a comparison with an $O(a)$-improved light quark calculation. The matching between the top two lattice spacings is the calculation described in this paper.

in a calculation now on the larger volume. The first same-physical-volume matching of the energy spectrum is done between the heavy quark theory and a conventional fine-lattice calculation done with domain wall fermions. An example of this finite-volume, step-scaling recursion is shown in Fig. 1.

Specifically, we will calculate the pseudoscalar (PS), vector (V), scalar (S), and axial-vector (AV) meson masses in the heavy-heavy (hh) system and pseudoscalar and vector masses for the heavy-light (hl) system. We will work with the following mass combinations:

(i) Spin-average: $m^{\mathrm{hh}}_{\mathrm{sa}} = \frac{1}{4}(m^{\mathrm{hh}}_{\mathrm{PS}} + 3m^{\mathrm{hh}}_{\mathrm{V}})$, $m^{\mathrm{hl}}_{\mathrm{sa}} = \frac{1}{4} \times (m^{\mathrm{hl}}_{\mathrm{PS}} + 3m^{\mathrm{hl}}_{\mathrm{V}})$

(ii) Hyperfine splitting: $m^{\mathrm{hh}}_{\mathrm{hs}} = m^{\mathrm{hh}}_{\mathrm{V}} - m^{\mathrm{hh}}_{\mathrm{PS}}$, $m^{\mathrm{hl}}_{\mathrm{hs}} = m^{\mathrm{hl}}_{\mathrm{V}} - m^{\mathrm{hl}}_{\mathrm{PS}}$

(iii) Spin-orbit average and splitting: $m^{\mathrm{hh}}_{\mathrm{soa}} = \frac{1}{4} \times (m^{\mathrm{hh}}_{\mathrm{S}} + 3m^{\mathrm{hh}}_{\mathrm{AV}})$, $m^{\mathrm{hh}}_{\mathrm{sos}} = m^{\mathrm{hh}}_{\mathrm{AV}} - m^{\mathrm{hh}}_{\mathrm{S}}$

(iv) Mass ratio: m_1/m_2 where $E^2 = m_1^2 + \frac{m_1}{m_2}p^2$, with m_1 the rest mass and m_2 the kinetic mass.

By examining these seven quantities we should be able to determine the three parameters $m_0 a$, ζ, and c_P and also check the size of the scaling violations.

The first step in this program calculates these seven quantities using the domain wall fermion action on the fine, $24^3 \times 64$ lattice with $1/a = 5.4$ GeV (I). Next, these seven quantities are computed a second time using a coarse, $16^3 \times 32$ lattice with $1/a = 3.6$ GeV and, therefore, the same physical volume. This is calculation II. The three heavy quark parameters entering this coarse-lattice calculation must be adjusted so that these seven quantities agree between calculations I and II. It is these calculations that are carried out in this paper using the parameters given in Table II.

Third, we expand the volume of calculation II to $24^3 \times 48$, while keeping all other parameters fixed. The results of this third, expanded volume calculation (III) can then be matched with a fourth calculation which has a lattice spacing larger by a factor of $3/2$ (IV). The simulation parameters for this second matching step are given in Table III. By repeating this pattern, we can extend the calculation to quenched lattices with the desired volume where serious, infinite-volume, charm physics may be studied.

TABLE II. The specific choice of parameters for the two sets of lattice configurations analyzed in this paper.

	I	II
Volume	$24^3 \times 48$	$16^3 \times 32$
$1/a$	5.4 GeV	3.6 GeV
L	0.9 fm	0.9 fm
β	6.638	6.351
ma	0.2	0.3
Action	DWF	RHQ

In this paper, we demonstrate only the matching between calculations I and II. The leading heavy quark discretization error in calculation I is of order $(ma)^2$ where $(ma)^2 \approx 4\%$, making it the dominant systematic error on the fine-lattice result. Of course, this error can be reduced in future calculations by choosing a fine lattice that has an even smaller lattice spacing and correspondingly smaller physical volume. Without improvement beyond the usual Sheikholeslami and Wohlert term, the leading heavy quark discretization error on the coarse lattice is expected to be $O(ma)^2$ with $(ma)^2 \approx 10\%$. However, once we introduce the improved lattice action of Eq. (1) and properly tune the coefficients, we should be able to reduce the error to $(a|\vec{p}|)^2 \approx 1\%$.

As will be demonstrated in the remainder of this paper, this proposed step-scaling method works well and offers a feasible approach to heavy quark calculations with accurately controlled finite lattice spacing errors. However, unless we can move beyond the quenched approximation used here, this method will be of only limited utility. Using this method for full QCD will, of course, be more computationally demanding because each of the two sets of lattice

TABLE III. The choice of parameters for the two sets of lattice configurations needed for the next step in this step-scaling program. Calculations with these parameters are now underway but are not described in this paper.

	III	IV
Volume	$24^3 \times 48$	$16^3 \times 32$
$1/a$	3.6 GeV	2.4 GeV
L	1.33 fm	1.33 fm
β	6.351	6.074
ma	0.3	0.45
Action	RHQ	RHQ

configurations generated for this matching process must be obtained from a full, dynamical simulation including the quark determinant. However, such an approach could become prohibitively expensive if the value of the light dynamical quark masses, $m_{\text{light}}a$, must decrease toward zero with decreasing a.

Fortunately, such small dynamical quark masses are not required in this step-scaling approach. The combination of the usual gauge and light quark action together with the effective lattice action of Eq. (1) defines a complete physical theory, including the properties of heavy quarks, that is unambiguously specified at short distances λ with $a \ll \lambda \ll 1/m_{\text{light}}$. Recall that in the continuum such a local field theory is typically defined in a mass- and volume-independent fashion. Short-distance renormalization conditions are imposed to fix the theory in a manner that is insensitive to quark masses and space-time volumes. Similarly our fine-lattice theory, viewed as a function of the bare input lattice parameters, also defines such a mass- and volume-independent theory.

Given sufficient computer power, the implications of this theory could be worked out on arbitrarily large spatial volumes and for arbitrarily small masses. The results would be well-defined functions of the bare input parameters which would require no adjustment as the quark mass and spatial volume were varied. The lattice spacing could be determined in physical units by comparing to Λ_{QCD} as determined from a vertex function at short distances with the light quark masses having a negligible effect.

Replacing the standard light quark action appropriate for our finest lattice with the improved lattice action of Eq. (1) does not change this situation. The parameters in the heavy quark action could be evaluated or renormalized by examining Green's functions evaluated at nonexceptional momenta without infrared or light quark mass sensitivity [24,29]. We would still be working with a short-distance-defined field theory that will give meaningful predictions as a function of lattice volume and light quark mass. Thus, when comparing two such effective theories defined at two different lattice spacings we are free to use any lattice size L and dynamical quark mass m_{light} we find convenient provided $L \gg a$ and $m_{\text{light}} \ll 1/a$. In fact, if m_{light} is sufficiently small that it does not effect the finite-volume heavy quark spectrum being compared, we need not even use the same quark mass in the two calculations being compared! Of course, this is likely a quark mass that is expensively small and a better strategy is to work with sufficiently small spatial volume and sufficiently heavy dynamical quark mass that they do effect the quantities being matched and must be given equivalent physical values in each of the calculations being compared.

We conclude that employing the procedure developed here in full QCD, while difficult, is practical and well within the reach of present computer resources. Just as our step-scaled lattice spacing decreases and we move to increasingly smaller spatial volumes, we should also move to increasingly heavier quark masses. In both cases finite volume and finite dynamical quark mass effects are distorting the spectrum being compared, but these distortions are entirely physical and must be accurately described by the effective actions being compared.

III. SIMULATIONS

We performed this calculation on a 512-node partition of the QCDOC machine located at Columbia University. We used the Wilson gauge action since for this case the relation between lattice coupling and lattice spacing has been thoroughly studied [30,31].

The gauge configurations were generated using the heat-bath method of Creutz [32], adapted for SU(3) using the two-subgroup technique of Cabibbo and Marinari [33]. The first 20 000 sweeps were discarded for thermalization and configurations thereafter were saved and analyzed every 10 000 sweeps. We examined the autocorrelation between configurations for both the standard 4-link plaquette and the hadron propagators evaluated at a time separation of 12 lattice units. Here we use the standard autocorrelation function $\rho(t)$ as

$$\rho(t) = \frac{1}{N_{\text{tot}} - t} \sum_{j}^{N_{\text{tot}}-t} (O(j) - \bar{O})(O(t+j) - \bar{O}) \qquad (5)$$

and identify the autocorrelation time as the size of the region near $t = 0$ in which $\rho(t) \neq 0$.

For the case of the plaquette (which was calculated every sweep), we found an autocorrelation time of approximately 3 sweeps. We studied the propagator correlations using two $24^3 \times 32$, $\beta = 6.638$ test calculations: in the first, the propagators were computed on 120 configurations, separated by 5 sweeps and in the second on 40 configurations separated by 50 sweeps. The resulting correlation functions for five different hadron propagators evaluated at a temporal source-sink separation of 12 lattice units are shown in Fig. 2. Autocorrelation on the scale of 100 sweeps can be seen in the data sampled every five sweeps. Essentially no autocorrelation can be seen for the propagators sampled every 50 sweeps. Since we used a total of 100 such lattice configurations, separated by 10 000 sweeps, for all of the quantities discussed in this paper, we will assume that quantities calculated on different configurations are statistically independent.

A. Lattice scale

Four different quantities with a meaningful physical scale enter each of the two lattice calculations that must be matched at a given stage in our step-scaling procedure. Most familiar is the distance scale determined by the static quark potential or the chiral limit of the light hadron spectrum. This is an important physical scale that will influence even small-volume, heavy quark results. As is

conventional, we will refer to this quantity as the "lattice spacing." (For example, we might determine the Compton wave length of the ρ meson to be 2.5 lattice units. This would yield a lattice spacing $a = \lambda_\rho/2.5 = 0.26\ \text{fm}/2.5 = 0.105\ \text{fm}$.) We will find it convenient to determine this from direct calculation of the static quark potential. The other three scales are the lattice volume, and the masses of the light and heavy quarks. (In our discussion of heavy-light systems we will ignore the strange quark and work with degenerate up and down quarks.)

Of course, the lattice spacing, expressed in physical units, is also important since it gives us a direct idea of the size of the discretization errors which we are trying to control. For this purpose we do not need great precision (something that cannot be achieved in a quenched calculation under any circumstances). We will determine the lattice spacing in physical units from the static quark potential evaluated at an intermediate distance to yield the Sommer scale [30] which is then determined from a phenomenological, static quark potential model. While the later is not precisely defined, this method has the advantage that it uses only pure gauge theory without any fermion action being involved. We could get a physical value for the lattice scale from the pion decay constant f_π or the rho meson mass but these are more difficult to calculate and may be more sensitive to finite volume and other systematic errors.

Our strategy for choosing the parameters to be used on the fine lattice and then finding physically equivalent parameters to be used on the coarser lattice proceeds as follows. We first decide on a target ratio of lattice scales determined by the ratio of lattice volumes that we intend to use. In the present case a ratio of $3/2$ is implied by our choice of 24^3 and 16^3 lattice volumes. Second, we choose the bare lattice coupling on the fine lattice to ensure that the fine-lattice spacing is sufficiently small (here chosen to be

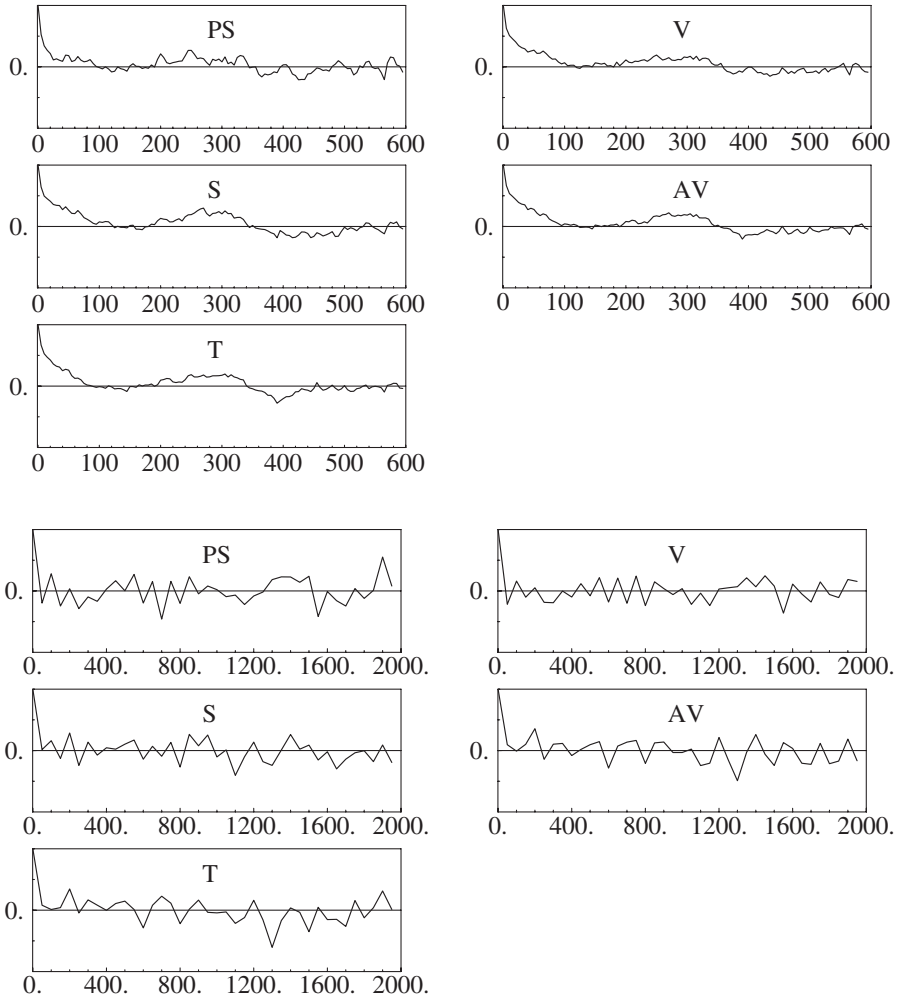

FIG. 2. The autocorrelation function for five different heavy-heavy meson propagators evaluated at a source-sink separation of 12 lattice units with $\beta = 6.638$ and a $24^3 \times 48$ space-time volume. In the top graph the propagators were calculated on every 5th configuration while in the bottom graph the propagator measurements were separated by 50 sweeps. This suggests that our separation of 10 000 sweeps between measurements ensures that they will be uncorrelated.

$1/a = 5.4$ GeV). The stronger coupling must then give a lattice spacing larger by a factor of $3/2$ than the fine value or $1/a = 3.6$ GeV. While for a dynamical QCD calculation, this would require considerable numerical exploration, for a quenched calculation with the Wilson gauge action, we can simply refer to extensive earlier work.

Next we choose the light quark mass to be used on the fine lattice as sufficiently light that the heavy-light mesons being studied will involve a different momentum scale than do the heavy-heavy mesons but not so light as to unreasonably increase the computational cost. For the calculations reported here we used the domain wall formalism for the light quarks and chose the mass $m_f a = 0.02$, one-tenth of the 0.2 heavy quark mass. The light quark mass to be used on the coarse lattice is determined by requiring that the light-light pseudoscalar meson have a mass $3/2$ times larger than that found on the fine lattice when measured in lattice units.

Finally the heavy quark mass on the fine lattice is estimated to correspond to the bare charm-quark mass. While in the present calculation we have used the single value $m_f a = 0.2$, a complete calculation will likely require one or two more masses so that a final interpolation/extrapolation can be done to make the physical charmed hadron mass agree with experiment. The heavy quark mass on the coarse lattice is one of the three heavy quark parameters whose determination is discussed in the next section.

Let us now discuss the choice of lattice scale in more detail. The static potential is expected to have the following form:

$$V(R) = C - \frac{\alpha}{R} + \sigma R, \tag{6}$$

where R is the separation between the static quarks. The scale implied by the heavy quark potential is often specified using the Sommer parameter r_0 which is defined by the condition

$$-R^2 \frac{\partial V(R)}{\partial R}\bigg|_{R=r_0} = 1.65. \tag{7}$$

This is appropriate on standard size lattices for bare couplings in the range $\beta = 6/g^2 \leq 6.57$. For weaker couplings, $\beta > 6.57$, one uses a second, smaller distance scale r_c defined by

$$R^2 F(R)|_{R=r_c} = 0.65, \tag{8}$$

where $\frac{r_c}{r_0} = 0.5133(24)$ [31]. While it may be problematic in a quenched calculation, we can attempt to determine r_0 from a phenomenological potential model, which gives $r_0 = 0.5$ fm [34].

Reference [31] gives predictions for the resulting lattice spacing when the coupling β of Wilson gauge action is in the range $5.7 \leq \beta \leq 6.92$:

$$\ln(a/r_0) = -1.6804 - 1.7339(\beta - 6) + 0.7849(\beta - 6)^2 - 0.4428(\beta - 6)^3. \tag{9}$$

With the help of Eq. (9), we can locate the β values needed to achieve the desired cutoff scales and fine-tune it later as necessary. As our final choices, we have $\beta = 6.638$ for the $a^{-1} = 5.4$ GeV lattice and $\beta = 6.351$ for the $a^{-1} = 3.6$ GeV one.

Since the comparison of lattice scales between our two simulations is fundamental to this matching program, we have carried out additional calculations to make sure that the lattice spacing is correctly selected. This requires a direct calculation of the static quark potential on our lattice configurations.

Recall that the static quark potential can be extracted from the ratio of Wilson loops:

$$V(\vec{r}) = \log\left[\frac{\langle W(\vec{r}, t)\rangle}{\langle W(\vec{r}, t+1)\rangle}\right], \tag{10}$$

where $\langle \cdots \rangle$ denotes an average over gauge configurations. In order to improve the signal and to extract the potential $V(r)$ from smaller time separations, we smear the gauge links in the spatial directions according to Ref. [35]:

$$U_k(n) \rightarrow P_{\mathrm{SU(3)}}\Big[U_k(n) + c_{\mathrm{smear}} \sum_{l \neq k} U_l(n) U_k(n + \hat{l}) \times U_{-l}(n + \hat{l} + \hat{k})\Big], \tag{11}$$

where k and l each indicate a spatial direction, $P_{\mathrm{SU(3)}}$ is an operator that projects a link back to an SU(3) special unitary matrix, c_{smear} is the smearing coefficient (set to 0.5 in our case), and the smearing procedure is performed n_{smear} times. More details regarding the algorithm can be found in Refs. [36,37]. In our calculation we found good results for $n_{\mathrm{smear}} = 180$ for the fine lattice and $n_{\mathrm{smear}} = 60$ for the coarse one.

While we did determine the two scale standards r_0 and r_c individually for both of our lattice spacings, our lattice volumes are somewhat small to permit a comparison with infinite-volume results. We therefore also determined the ratio of lattice spacings without using the Sommer scale by directly comparing the potentials computed on our two sets of lattice configurations using the relation

$$V_1(n) = V_2(n/\lambda)/\lambda + C', \tag{12}$$

where $\lambda = a_2/a_1$ is the ratio of the two lattice spacings. We first fit the static potential on the fine lattice to the form given in Eq. (6), determining the parameters C, α, and σ. Next we scaled the resulting fitted function according to Eq. (12) and adjusted the parameters λ and C' in that equation to obtain the best fit to the static potential measured on the coarse lattice. Figure 3 shows a comparison of the potential determined from $\beta = 6.351$ configurations and a scaled and shifted version of the $\beta = 6.638$ poten-

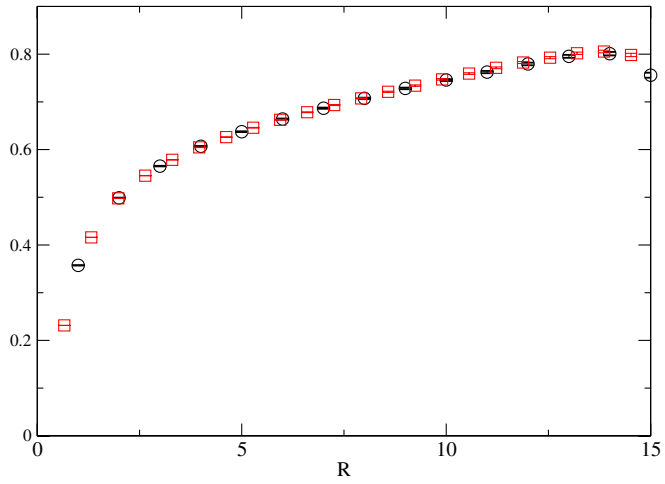

FIG. 3 (color online). The static quark potential calculated on both the coarse and fine lattices. The static quark potential values computed on the $\beta = 6.351$ lattice are shown as circles. The squares mark the static quark potential from the $\beta = 6.638$ lattice scaled by the fitted ratio of lattice spacings $\lambda = 1.51$ and shifted by a constant. The agreement between these two different sets of points gives good evidence that the ratio of lattice spacings between these two β values is the desired 3/2.

tial. The agreement is excellent and this procedure gives an independent value for the lattice spacing ratio of 1.51(2), which agrees with what we wanted.

B. Domain wall fermions

We will now briefly describe the domain wall fermion calculations that were used for the heavy quark on the finest lattice and the light quarks on both lattices. The domain wall Dirac operator can be written as

$$D_{x,s;x',s'} = \delta_{s,s'} D^{\parallel}_{x,x'} + \delta_{x,x'} D^{\perp}_{s,s'} \tag{13}$$

$$D^{\parallel}_{x,x'} = \frac{1}{2}\sum_{\mu=1}^{4}[(1-\gamma_\mu)U_{x,\mu}\delta_{x+\hat{\mu},x'} + (1+\gamma_\mu)U^{\dagger}_{x',\mu}\delta_{x-\hat{\mu},x'}] + (M_5 - 4)\delta_{x,x'} \tag{14}$$

$$D^{\perp}_{s,s'} = \frac{1}{2}[(1-\gamma_5)\delta_{s+1,s'} + (1+\gamma_5)\delta_{s-1,s'} - 2\delta_{s,s'}] - \frac{m_f a}{2}[(1-\gamma_5)\delta_{s,L_s-1}\delta_{0,s'} + (1+\gamma_5)\delta_{s,0}\delta_{L_s-1,s'}], \tag{15}$$

where the fifth-dimension indices s and s' lie in the range $0 \le s, s' \le L_s - 1$, M_5 is the five-dimensional mass, and m_f directly couples the two walls at $s = 0$ and $s = L_s - 1$. It is related to the physical mass of the four-dimensional fermions.

The M_5 parameter is optimized by the choice of $M_5 \approx 1 - m_{\text{crit}}$, where m_{crit} is the critical value of the mass for the 4-dimensional Wilson fermion action. This quantity has been calculated perturbatively up to one-loop level for the Wilson gauge action and either the Wilson [38] or SW [39] fermion actions. In the quenched approximation, for Wilson fermions and with our choices of gauge coupling, we find $m_{\text{crit}} = -0.495$ at $\beta = 6.638$, and $m_{\text{crit}} = -0.522$ at $\beta = 6.351$. Therefore, we use $M_5 = 1.5$ in the DWF action for both our β values.

The DWF action is $O(a)$ off-shell improved due to the preservation of chiral symmetry, and no further improvement in the action or quark fields is performed. The chiral symmetry breaking can be measured from the residual mass, which can be computed from the ratio

$$am_{\text{res}} = \frac{\sum_x \langle J^a_{5q}(\vec{x}, t)\pi(0)\rangle}{\sum_x \langle J^a_5(\vec{x}, t)\pi(0)\rangle}, \tag{16}$$

provided $t \gg a$. Here J_{5q} is a pseudoscalar density located at the midpoint of the fifth dimension. The residual mass has been thoroughly studied, for example, in Ref. [40] for various values of β, L_s, and M_5. Those results suggest that the m_{res} values for each of our lattice configurations are much smaller than the 0.001 24 value determined at $\beta = 6.0$ with lattice volume $16^3 \times 32 \times 16$ and $M_5 = 1.8$. This indicates that chiral symmetry breaking is small, and ignoring the contribution of m_{res} in the heavy quark sector will have an effect smaller than 0.5%.

However, there is a limitation to using large values of m_f with DWF. Recall that there are two types of eigenvectors of the Hermitian DWF Dirac operator: propagating and decaying states [41,42]. The former, unphysical states have nonzero 5th-dimension momenta and large Dirac eigenvalues around $1/a$. The "decaying" states are bound to the walls of the 5th dimension and are the physical states corresponding to the four-dimensional Dirac eigenstates in the continuum limit. The gap between these two types of states is controlled by the domain wall height M_5. However, as m_f increases, the eigenvalues of the physical states increase while those of the propagating states do not. Thus, we must be careful to avoid the situation in which the states with the smallest eigenvalues are dominated by these unphysical states. Therefore, a careful check on the lowest eigenvalues for the target m_f being used to simulate the heavy quarks on the fine lattice is needed. Figure 4 shows the 5-dimensional eigenfunction, averaged over 4-dimensional space, $\sum_x |\Psi_{x,s}|^2$ as a function of the 5th-dimensional coordinate s for the lowest 19 eigenvalues with various $m_f a$: 0.22, 0.27, 0.37, 0.47. As can be seen in the figure, these first 19 eigenfunctions appear to be physical states bound to the 4-dimensional wall for the first three mass values. However, $m_f a = 0.47$ is sufficiently large that propagation into the 5-dimension can be clearly seen. We conclude that our $m_f a = 0.2$ for the heavy quark is safe, well below the region where such unphysical states arise.

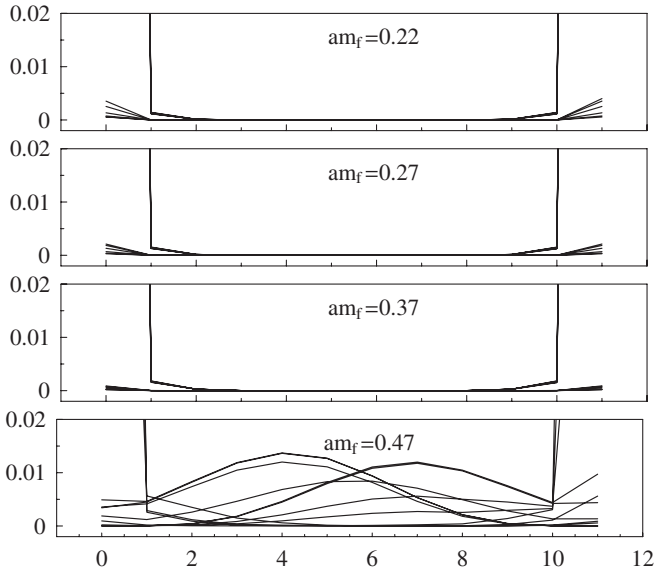

FIG. 4. The dependence on the fifth dimension, s, of the space-time sum of the modulus squared of the 19 lowest-lying eigenvectors of the Hermitian domain wall Dirac operator: $\sum_x |\Psi_{x,s}|^2$. This is shown for a Wilson quenched gauge configuration with $\beta = 6.638$, $V = 16^4$, $L_s = 12$, $M_5 = 1.8$, and $m_f a \in \{0.22, 0.27, 0.37, 0.47\}$. The unphysical, propagating states are seen only for $m_f a > 0.37$.

C. Spectrum measurements

In order to get good signals for the heavy quark states of interest for relatively small time separations, a smeared wave function source is used for the heavy quark (but not the light quark). Here, we adopt the Coulomb gauge-fixed hydrogen ground-state wave function,

$$\Psi_{gnd}(r) = e^{-r/r_0}, \tag{17}$$

as the source of the heavy fermion(s) and use a point source for the light fermion (if any). At the sink the two propagators are evaluated at the same point and the resulting gauge invariant combination summed over a 3-dimensional plane at fixed time, with a possible momentum projection factor. An optimized radius, r_0, was chosen in the fashion suggested in Ref. [43]. Table IV lists all the local meson operators used in our calculation.

TABLE IV. Meson states created by local operators of the form $\bar{\psi}\Gamma\psi$, labeled in spectroscopic notation.

Γ	$^{2S+1}L_J$	J^{PC}
γ_5	$^1S_0$	0^{-+}
γ_i	$^3S_1$	1^{--}
1	$^3P_0$	0^{++}
$\gamma_5\gamma_i$	$^3P_1$	1^{++}

Figure 5 shows how the plateau in the effective mass plot improves between a point and smeared source. The smeared-source meson plateaus are much better than those of the local source, even for the scalar and axial-vector mesons.

To constrain the space-time asymmetry parameter ζ, we also computed the pseudoscalar meson energy in the heavy-heavy sector for the three lowest momenta: $\frac{2\pi}{L} \times (0, 0, 0)$, $\frac{2\pi}{L}(0, 0, 1)$, and $\frac{2\pi}{L}(0, 1, 1)$, where L is the spatial lattice size. The dispersion relation may be expanded in momentum as

$$E(p) = m_1 + \frac{p^2}{2m_2} + O(p^4). \tag{18}$$

As we will see, requiring the ratio of static to kinetic mass, $m_2/m_1 = 1$, is useful for determining the coefficient ζ.

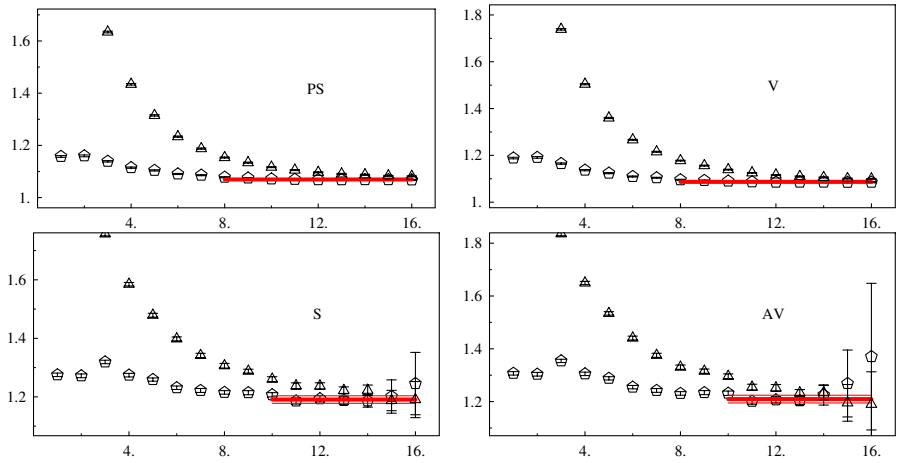

FIG. 5 (color online). A comparison of effective mass plateaus between point and smeared sources in the heavy-heavy sector. Triangles denote the point-point source, and pentagons denote the point-smeared heavy meson correlators. Clearly, the plateaus have been improved by the smearing. However, a double-cosh fit to the two distinct wave function sources might help us determine the ground-state energy even more accurately.

TABLE V. Common parameters for each of the coarse and fine data sets. For both data sets $L = 0.9$ fm, while for the domain wall fermion action we use $L_s = 12$ and $M_5 = 1.5$. Here "TBD" indicates a value to be determined in the matching procedure being developed here.

Label	β	V	S_L	am_L	S_H	am_H	a^{-1} (static quark potential)
Fine	6.638	$24^3 \times 48$	DWF	0.02	DWF	0.2	5.4 GeV
Coarse	6.351	$16^3 \times 32$	DWF	0.03	RHQ	TBD	3.6 GeV

TABLE VI. Mass spectrum measured on the fine lattice in units of a^{-1}.

	m_{PS}	m_{V}	m_1/m_2	m_{AV}	m_{S}
Light-light	0.175(3)	0.233(5)	...	...	...
Heavy-light	0.467(2)	0.485(3)	...	...	...
Heavy-heavy	0.716(1)	0.728(1)	1.02(2)	0.810(5)	0.799(4)

D. Parameters

Table V lists the fixed parameters used throughout this matching stage for the fine and coarse lattices. The heavy quark mass was set to approximate that of the charm mass and the light quark mass was chosen 10 times smaller. The lattice spacing ratio between these two lattices is 1.5. The domain wall fermion parameters used on the fine lattice have been carefully studied and we find no unphysical states in the chosen mass range as discussed in previous section. Table VI shows the hadron mass spectrum computed on the fine lattice. As can be seen, $m_1/m_2 = 1.02(2)$ is consistent with 1, indicating that heavy quark discretization effects using domain wall fermions are small. One expects that the light quark mass on the coarse lattice should be 0.03 and the data for the light-light spectrum with this choice of light quark mass is listed in Table VII. As one can see from Table VII, the light-light meson spectra on the coarse and fine lattices agree when compared in the same units, indicating that the light quark mass is well tuned on the coarse lattice.

A complete list of the parameter sets used for the RHQ action on the coarse lattice is given in Table VIII. The first 42 sets of data were initial trials chosen to give good coverage in parameter space. In order to perform a more systematic analysis, described in Sec. IV, we also collected a "Cartesian" set (sets Nos. 43–66) chosen close to the desired fine-lattice measurements. These 24 data sets are centered around set No. 14. The range of each parameter in this Cartesian data set was selected so that within that range the estimated difference between a linear and qua-

TABLE VII. Light-light hadron spectrum measured on the coarse lattice in units of a^{-1} and units of $3/2a$ to compare with the fine-lattice results in Table VI.

	Units	m_{PS}	m_{V}
Light-light	$1/a$	0.259(6)	0.328(10)
Light-light	$3/2a$	0.173(4)	0.219(7)

TABLE VIII. Parameters used on the coarse lattice.

Set number	$m_0 a$	c_B	c_E	ζ
1	0.0	1.552 06	1.457 69	1.012 81
2	0.07	1.5474	1.424 45	1.000 63
3	0.0426	1.550 34	1.438 43	1.006 74
4	0.0426	1.550 34	1.438 43	1.1
5	0.0426	1.550 34	1.438 43	0.9
6	0.033 002 9	1.609 21	1.538 43	1.043 95
7	0.023 002 9	1.609 21	1.438 43	1.043 95
8	0.023 002 9	1.609 1	1.538 43	1.043 95
9	0.0426	1.609 21	1.438 43	1.043 95
10	0.0426	1.550 34	1.438 43	1.006 74
11	0.	1.552 06	1.438 43	1.012 81
12	0.032 789 3	1.5108 1	1.438 43	1.035 63
13	0.023 002 9	1.510 81	1.438 43	1.035 63
14	0.032 789 3	1.510 81	1.538 43	1.035 63
15	0.01	1.700 12	1.574 29	1.021 52
16	0.003 705	1.708 62	1.5768	1.023 49
17	0.0138	1.714 95	1.578 71	1.024 99
18	0.02	1.718 86	1.579 91	1.025 93
19	0.03	1.725 23	1.581 88	1.027 49
20	0.08	1.706 83	1.576 27	1.023 07
21	0.09	1.713 08	1.578 15	1.0245
22	0.1	1.719 39	1.580 07	1.026 06
23	0.101 197	1.5031	1.932 37	1.003 17
24	0.159 393	1.456 19	2.426 73	0.999 347
25	0.217 59	1.409 29	2.9211	0.995 52
26	0.275 786	1.362 38	3.415 47	0.991 694
27	0.333 983	1.315 48	3.909 83	0.987 867
28	0.392 179	1.268 58	4.4042	0.984 041
29	−0.132 144	1.963 91	0.619 831	1.047 58
30	−0.064 219 7	1.836 27	1.098 32	1.035 53
31	−0.030 257 3	1.772 44	1.337 56	1.029 51
32	−0.009 879 93	1.734 15	1.4811	1.0259
33	0.017 289 9	1.683 09	1.6725	1.021 08
34	0.037 667 3	1.6448	1.816 04	1.017 47
35	0.043 216	1.5843	0.635 194	1.044 15
36	0.027 915 7	1.621 66	1.490 05	1.043 85
37	0.038 103	1.596 76	1.586 81	1.044 05

TABLE VIII. (*Continued*)

Set number	m_0a	c_B	c_E	ζ
38	0.022 841 3	1.634 12	1.441 67	1.043 75
39	0.012 445 8	1.7295	1.235 41	1.042 95
40	0.012 445 8	1.7295	1.615 02	1.042 95
41	0.012 445 8	1.7295	0.855 798	1.042 95
42	0.027 386	1.709 23	1.307 37	1.038 74
43	0.132 789	1.610 81	1.838 43	1.055 63
44	−0.067 210 7	1.610 81	1.838 43	1.055 63
45	0.132 789	1.410 81	1.838 43	1.055 63
46	−0.067 210 7	1.410 81	1.838 43	1.055 63
47	0.132 789	1.610 81	1.238 43	1.055 63
48	−0.067 210 7	1.610 81	1.238 43	1.055 63
49	0.132 789	1.410 81	1.238 43	1.055 63
50	−0.067 210 7	1.410 81	1.238 43	1.055 63
51	0.132 789	1.610 81	1.838 43	1.015 63
52	−0.067 210 7	1.610 81	1.838 43	1.015 63
53	0.132 789	1.410 81	1.838 43	1.015 63
54	−0.067 210 7	1.410 81	1.838 43	1.015 63
55	0.132 789	1.610 81	1.238 43	1.015 63
56	−0.067 210 7	1.610 81	1.238 43	1.015 63
57	0.132 789	1.410 81	1.238 43	1.015 63
58	−0.067 210 7	1.410 81	1.238 43	1.015 63
59	0.132 789	1.510 81	1.538 43	1.035 63
60	−0.067 210 7	1.510 81	1.538 43	1.035 63
61	0.032 789 3	1.610 81	1.538 43	1.035 63
62	0.032 789 3	1.410 81	1.538 43	1.035 63
63	0.032 789 3	1.510 81	1.838 43	1.035 63
64	0.032 789 3	1.510 81	1.238 43	1.035 63
65	0.032 789 3	1.510 81	1.538 43	1.055 63
66	0.032 789 3	1.510 81	1.538 43	1.015 63

dratic fit would be less than 5% as expected from an examination of the first 42 parameter sets. This yields a region that is close to reproducing the target fine data and in which a linear approximation should be good: $m_0a = 0.0328 \pm 0.1$, $c_B = 1.511 \pm 0.1$, $c_E = 1.538 \pm 0.3$ and $\zeta = 1.036 \pm 0.02$, which is shown in Fig. 6.

The 24-set Cartesian data will allow us to calculate the first and second derivatives directly from the measurements. Note that we have more measurements than we actually need. This provides additional checks on our method and the validity of the scaling of physical quantities between the coarse and fine lattices. We expect that the total number of data sets that we will use for the next step of matching will be dramatically reduced.

Using the methods described in Sec. III C, we have measured the pseudoscalar (PS), vector (V), scalar (S), and axial-vector (AV) mesons in the heavy-heavy system, and PS and V in the heavy-light system. We use combinations of the masses to try to simplify their dependence on the coefficients of the RHQ action. For the heavy-light system, we use the spin-average and hyperfine splitting; for the heavy-heavy system, we use these and also include the spin-orbit average, spin-orbit splitting, and the ratio of

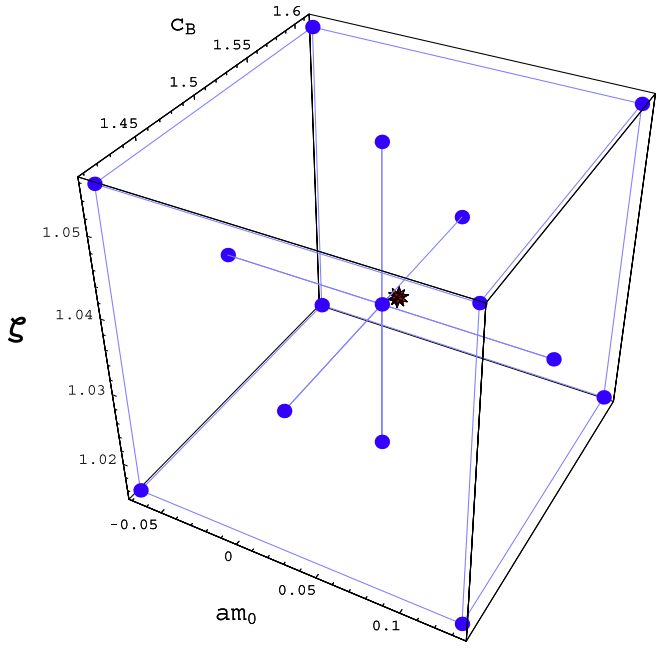

FIG. 6 (color online). The distribution in the 3-parameter space (m_0a, c_B, ζ) of the 24-set Cartesian data. The center circular point is set No. 14, and the points around it are sets Nos. 43–66. The starred point represents the final matching coefficients determined in Sec. IV B.

m_1/m_2. The resulting values for these quantities for each of the 66 data sets are given in Table IX.

IV. ANALYSIS AND RESULTS

The final step in this matching procedure is to determine the parameters in the heavy quark action of Eq. (1), $\{m_0a, c_B, c_E, \zeta\}$, that will yield the seven quantities measured on the coarse lattice which agree with those determined on the fine lattice. Of course, this might be done by "trial and error" and, as can be seen by scaling the numbers in Table IX, data set No. 14 comes very close to such a result. However, to fully understand this step-scaling method (for example to properly propagate errors), it is important to learn in detail how the measured spectra depend on these input parameters.

As a starting point, we will attempt to use a subset of our parameter space chosen so that the resulting coarse-lattice hadron masses are well fit by a simple linear dependence on the heavy quark parameters:

$$Y^n = A + J \cdot X^n, \tag{19}$$

where n labels the parameter set while X and Y are 4-dimensional and 7-dimensional column vectors made up of the four input heavy-action parameters and the seven computed masses or mass ratios, respectively:

TABLE IX. Mass spectrum measured on the coarse lattice in units of a^{-1} (where "sa" is spin averaged, "hs" is hyperfine splitting, "soa" is spin-orbit averaged, "sos" is spin-orbit splitting; "hl" is heavy-light and "hh" is heavy-heavy).

Set number	$m_{\mathrm{sa}}^{\mathrm{hh}}$	$m_{\mathrm{hs}}^{\mathrm{hh}}$	$m_{\mathrm{sa}}^{\mathrm{hl}}$	$m_{\mathrm{hs}}^{\mathrm{hl}}$	$m_{\mathrm{sos}}^{\mathrm{hh}}$	$m_{\mathrm{soa}}^{\mathrm{hh}}$	m_1/m_2
1	1.0137(17)	0.0174(6)	0.679(5)	0.0254(17)	0.020(5)	1.135(14)	0.988(21)
2	1.1314(15)	0.0152(5)	0.742(4)	0.0221(15)	0.017(4)	1.251(13)	0.949(18)
3	1.0872(16)	0.0160(5)	0.718(5)	0.0233(15)	0.018(4)	1.207(14)	0.966(19)
4	1.1755(16)	0.0153(5)	0.762(5)	0.0228(15)	0.017(4)	1.298(13)	1.075(21)
5	0.9776(16)	0.0169(5)	0.664(5)	0.0241(16)	0.020(5)	1.094(14)	0.842(16)
6	1.0724(17)	0.0171(5)	0.709(5)	0.0248(16)	0.019(5)	1.193(14)	1.021(21)
7	1.0840(15)	0.0170(5)	0.716(4)	0.0246(16)	0.018(4)	1.208(12)	1.009(17)
8	1.0622(15)	0.0176(5)	0.704(4)	0.0254(16)	0.025(4)	1.190(12)	1.016(18)
9	1.1177(15)	0.0165(5)	0.734(4)	0.0238(15)	0.017(4)	1.241(12)	1.002(16)
10	1.0949(14)	0.0161(5)	0.723(4)	0.0234(15)	0.017(4)	1.217(12)	0.956(15)
11	1.0255(15)	0.0174(5)	0.686(4)	0.0254(16)	0.019(4)	1.149(12)	0.980(17)
12	1.1148(15)	0.0157(5)	0.733(4)	0.0232(15)	0.017(4)	1.238(12)	0.992(16)
13	1.0981(15)	0.0160(5)	0.724(4)	0.0236(15)	0.017(4)	1.221(12)	0.995(16)
14	1.0937(15)	0.0162(5)	0.721(4)	0.0239(15)	0.018(4)	1.216(12)	0.998(16)
15	0.9384(19)	0.0204(7)	0.638(5)	0.0287(19)	0.024(6)	1.060(15)	1.016(23)
16	0.9637(18)	0.0199(6)	0.652(5)	0.0280(18)	0.023(5)	1.085(15)	1.013(23)
17	0.9822(18)	0.0195(6)	0.661(5)	0.0275(18)	0.022(5)	1.103(15)	1.012(22)
18	0.9935(18)	0.0193(6)	0.667(5)	0.0273(18)	0.022(5)	1.114(14)	1.011(22)
19	1.0115(18)	0.0190(6)	0.677(5)	0.0268(17)	0.021(5)	1.132(14)	1.009(22)
20	1.1019(16)	0.0171(5)	0.725(5)	0.0242(16)	0.019(5)	1.221(13)	0.986(20)
21	1.1187(16)	0.0169(5)	0.734(5)	0.0239(16)	0.018(4)	1.237(13)	0.985(19)
22	1.1353(16)	0.0167(5)	0.743(5)	0.0235(15)	0.018(4)	1.254(13)	0.984(19)
23	1.0809(16)	0.0164(5)	0.714(5)	0.0240(16)	0.019(5)	1.196(14)	0.973(19)
24	1.0521(16)	0.0175(6)	0.699(5)	0.0255(16)	0.020(5)	1.164(14)	0.988(20)
25	0.9985(17)	0.0195(6)	0.670(5)	0.0279(18)	0.023(6)	1.107(14)	1.013(22)
26	0.9143(19)	0.0229(8)	0.624(5)	0.0318(20)	0.027(7)	1.021(15)	1.054(27)
27	0.7896(23)	0.0295(11)	0.557(5)	0.0384(25)	0.035(9)	0.895(18)	1.12(4)
28	0.606(3)	0.0469(28)	0.460(6)	0.052(4)	0.053(18)	0.708(24)	1.21(10)
29	0.8593(22)	0.0235(8)	0.596(5)	0.0316(21)	0.026(7)	0.993(17)	1.049(28)
30	0.9229(20)	0.0212(7)	0.630(5)	0.0293(19)	0.024(6)	1.050(15)	1.027(25)
31	0.9461(19)	0.0204(7)	0.642(5)	0.0286(19)	0.023(6)	1.070(15)	1.019(24)
32	0.9573(19)	0.0201(7)	0.648(5)	0.0282(18)	0.023(6)	1.079(15)	1.016(23)
33	0.9693(18)	0.0197(6)	0.655(5)	0.0279(18)	0.023(5)	1.089(15)	1.011(23)
34	0.9760(18)	0.0195(6)	0.658(5)	0.0277(18)	0.023(5)	1.095(14)	1.009(22)
35	1.2455(15)	0.0136(4)	0.802(4)	0.0195(13)	0.013(4)	1.372(13)	0.976(18)
36	1.0711(17)	0.0171(5)	0.708(5)	0.0248(16)	0.019(5)	1.192(14)	1.020(21)
37	1.0736(17)	0.0170(5)	0.709(5)	0.0248(16)	0.019(5)	1.194(14)	1.022(21)
38	1.0696(17)	0.0172(5)	0.707(5)	0.0248(16)	0.019(5)	1.191(14)	1.019(21)
39	1.0700(17)	0.0176(5)	0.708(5)	0.0249(16)	0.019(5)	1.194(14)	1.013(21)
40	0.9864(18)	0.0198(6)	0.663(5)	0.0279(18)	0.022(5)	1.108(15)	1.036(23)
41	1.1359(16)	0.0162(5)	0.743(5)	0.0228(15)	0.017(4)	1.262(13)	0.997(20)
42	1.0824(17)	0.0173(5)	0.715(5)	0.0245(16)	0.019(5)	1.205(14)	1.007(21)
43	1.1866(15)	0.0157(5)	0.769(4)	0.0227(15)	0.017(4)	1.303(13)	1.019(20)
44	0.8149(23)	0.0245(9)	0.571(5)	0.0340(23)	0.030(7)	0.937(17)	1.10(3)
45	1.2271(15)	0.0138(4)	0.790(4)	0.0209(14)	0.015(4)	1.344(13)	1.012(19)
46	0.8705(22)	0.0212(8)	0.601(5)	0.0309(21)	0.027(6)	0.993(16)	1.090(28)
47	1.3000(14)	0.0136(4)	0.830(4)	0.0195(13)	0.014(4)	1.420(12)	0.986(18)
48	0.9691(19)	0.0189(6)	0.654(5)	0.0274(18)	0.022(5)	1.095(15)	1.052(24)
49	1.3356(14)	0.0119(3)	0.849(4)	0.0179(12)	0.012(3)	1.456(12)	0.979(17)
50	1.0164(18)	0.0165(5)	0.679(5)	0.0250(17)	0.020(5)	1.143(14)	1.045(22)
51	1.1473(15)	0.0160(5)	0.749(4)	0.0230(15)	0.018(4)	1.263(13)	0.973(19)
52	0.7632(24)	0.0257(9)	0.545(5)	0.0354(24)	0.032(8)	0.884(17)	1.06(3)
53	1.1894(15)	0.0141(4)	0.772(4)	0.0210(14)	0.016(4)	1.305(13)	0.967(18)
54	0.8218(22)	0.0221(8)	0.576(5)	0.0319(21)	0.028(7)	0.943(16)	1.045(28)

TABLE IX. (*Continued*)

Set number	m_{sa}^{hh}	m_{hs}^{hh}	m_{sa}^{hl}	m_{hs}^{hl}	m_{sos}^{hh}	m_{soa}^{hh}	m_1/m_2
55	1.2662(14)	0.0138(4)	0.813(4)	0.0196(13)	0.014(4)	1.385(13)	0.940(17)
56	0.9272(19)	0.0194(6)	0.633(5)	0.0279(18)	0.023(6)	1.052(15)	1.004(23)
57	1.3030(14)	0.0120(3)	0.833(4)	0.0179(12)	0.013(3)	1.422(12)	0.934(17)
58	0.9764(18)	0.0169(6)	0.659(5)	0.0254(17)	0.020(5)	1.102(15)	0.997(21)
59	1.2495(15)	0.0137(4)	0.803(4)	0.0195(13)	0.014(4)	1.367(12)	0.978(18)
60	0.9026(20)	0.0200(7)	0.619(5)	0.0284(19)	0.023(6)	1.027(15)	1.052(24)
61	1.0626(17)	0.0172(5)	0.704(4)	0.0242(16)	0.018(5)	1.184(14)	1.016(20)
62	1.1071(17)	0.0151(5)	0.728(4)	0.0221(15)	0.016(4)	1.228(13)	1.009(19)
63	1.0140(18)	0.0179(6)	0.678(4)	0.0256(17)	0.020(5)	1.134(14)	1.034(21)
64	1.1453(16)	0.0148(5)	0.748(4)	0.0212(14)	0.015(4)	1.267(13)	0.995(19)
65	1.1051(17)	0.0160(5)	0.726(4)	0.0230(15)	0.017(4)	1.226(13)	1.036(20)
66	1.0656(17)	0.0163(5)	0.706(4)	0.0233(15)	0.017(4)	1.186(13)	0.989(19)

$$X = \begin{pmatrix} m_0 a \\ c_B \\ c_E \\ \zeta \end{pmatrix} \qquad Y = \begin{pmatrix} m_{sa}^{hh} \\ m_{hs}^{hh} \\ m_{sa}^{hl} \\ m_{hs}^{hl} \\ m_{soa}^{hh} \\ m_{sos}^{hh} \\ m_1/m_2 \end{pmatrix}. \tag{20}$$

The quantities A and J are a 7-dimensional column vector and a 7×4 matrix which represent the constant and linear terms in our linear approximation. (In most of the discussion to follow, we will work with all seven measured quantities. However, if this number is decreased, the vectors Y, A, and the matrix J will shrink appropriately.)

Given a specific group of N of our data sets, $X^{n_i}|_{1\le i\le N}$, we can determine the quantities A and J by minimizing an appropriate χ^2 for such a linear fit:

$$\chi^2_{\mathcal{C}} = \sum_{i=1}^{N} (A + J \cdot X^{n_i} - Y^{n_i})^T \cdot W_{\mathcal{C}}^{-1} \cdot (A + J \cdot X^{n_i} - Y^{n_i}). \tag{21}$$

Here W is a 7×7 matrix representing a choice of correlation matrix. In the results that follow we will use

$$(W_{\mathcal{C}})_{d,d'} = \sum_{i=1}^{N} \langle (Y_d^{n_i} - \bar{Y}_d^{n_i})(Y_{d'}^{n_i} - \bar{Y}_{d'}^{n_i}) \rangle, \tag{22}$$

where $\langle \cdots \rangle$ represents an average over the 100 jackknife blocks obtained by omitting one of the 100 measurements with $Y_d^{n_i}$ the result for that jackknife block and $\bar{Y}_d^{n_i}$ the corresponding average. Replacing $W_{\mathcal{C}}$ by the simpler, uncorrelated error matrix $(W'_{\mathcal{C}})_{d,d'} = \sum_{i=1}^{N} \delta_{d,d'} \sigma_d^{n_i}$ had little effect on the final results where σ_d^i is the usual squared error on the measured quantity Y_d^i. Determining the A and J which minimize $\chi^2_{\mathcal{C}}$ is straightforward because this is a quadratic function of these 35 numbers and the minimum can be obtained by solving 35 linear equations. Typically these 35 equations are quite regular, with a stable solution even if only a relative few of our data sets are used.

The use of linearity to determine the desired matching heavy quark parameters is reasonable if we are working in a region that is close to the right choice for those parameters. Once we have determined the matrix J and vector A, we can solve for the coefficients $X_{\mathcal{C}}$ that will yield meson masses equal to those found on the fine lattice, $Y_{\mathcal{F}}$. Here we add the subscripts $\mathcal{C}$ and $\mathcal{F}$ to indicate our estimates for the physical coarse-lattice parameters ($X_{\mathcal{C}}$) and the coarse-lattice masses ($Y_{\mathcal{F}}$), scaled from those calculated using the fine lattice.

Again we minimize a quantity $\chi^2_{\mathcal{F}}$, similar to that given in Eq. (20). However, the fine-lattice correlation matrix, $W_{\mathcal{F}}$, which appears in the equivalent version of Eq. (20) is defined through a modified version of Eq. (21). Specifically, the fine-data analogue of Eq. (21) is used for all but the seventh row and seventh column, which correspond to the quantity m_1/m_2. Since this must be unity in a relativistic calculation (and is one within errors for our DWF results), we set $(Y_{\mathcal{F}})_6 = 1$ and the corresponding elements of the correlation $(W_{\mathcal{C}})_{d\neq 6,6} = (W_{\mathcal{C}})_{6,d\neq 6} = 0$ for $0 \le d \le 6$. In order that the resulting correlation matrix be invertible, we arbitrarily set $(W_{\mathcal{C}})_{6,6} = 10^{-8}$. This has the effect of constraining the coarse-lattice value of $m_1/m_2 = 1$. The resulting minimum is again determined by solving a set of linear equations. That solution can be written explicitly as

$$X_{\mathcal{C}} = (J^T \cdot W_{\mathcal{F}}^{-1} \cdot J)^{-1} \cdot J^T \cdot W_{\mathcal{F}}^{-1} \cdot (Y_{\mathcal{F}} - A). \tag{23}$$

Finally, to determine the error on the resulting heavy quark parameters $X_{\mathcal{C}}$, we add in quadrature two different sources of error. To compute the first, we use the average value of the masses $Y_{\mathcal{F}}$, deduced from the fine-lattice calculation, which together with jackknifed results for J and A gives us the error on $X_{\mathcal{C}}$ coming from the statistical fluctuations in the coarse-lattice data. We then estimate the statistical error coming from the fine-lattice calculation by

using the average values for J and A in Eq. (22) and the jackknifed values of $Y_{\mathcal{F}}$ to determine the resulting fluctuations in the resulting heavy quark parameters $X_{\mathcal{C}}$ caused by the statistical errors in the determination of $Y_{\mathcal{F}}$.

A. Four-parameter action

As is suggested by the large number of data sets listed in Table VIII, we had greater difficulty than expected in determining the four parameters $m_0 a$, c_B, c_E, and ζ. Typically, reasonable choices of a subset of the parameter sets from the initial group of 42 parameter sets listed in Table VIII gave similar values for the final heavy quark parameters. However, the derivative matrix was typically quite singular and the resulting parameters, especially c_E, not well determined. In an attempt to make this process more deterministic, we collected the 24 Cartesian data sets from which we could determine the matrix of derivatives J from simple differences. The result for J agreed very well with that typically determined from the fitting procedure described earlier to the less regular parameter choices in our first 42 data sets. We conclude that this linear description of our coarse-lattice data is a good approximation. For simplicity, we present only the results from this final determination of J and A from the Cartesian data.

Specifically, the 24 parameter choices within our Cartesian data set (Nos. 43–66) use parameters of the form

$$X_i^n = \bar{X}_i + \sigma(n)_i \Delta_i. \tag{24}$$

Here the quantity $\{\sigma(n)_i\}_{0\le i\le 3}$ determines the first 16 parameter choices, where $\sigma(n)_i = (-1)^{\mathrm{int}(n/2^i)}$, the expression $\mathrm{int}(x)$ represents the integer part of the number x and the index n varies between 0 and 15. The four-parameter increments $\Delta_0 = 0.1$, $\Delta_1 = 0.1$, $\Delta_2 = 0.3$, and $\Delta_3 = 0.02$ were listed earlier and are displayed in Fig. 6. The remaining eight data sets use the values $\sigma(16+n)_i = (-1)^n \delta_{\mathrm{int}(n/2),i}$ for $n = 0, 1, \ldots, 7$. The quantities A and J can be directly determined using the following expressions:

$$J_{d,i} = \frac{1}{9} \sum_{n=0}^{23} \sigma(n)_i \frac{Y_d^n}{2\Delta_i} \tag{25}$$

$$A_d = \frac{1}{24} \sum_{n=0}^{23} Y_d^n - \sum_{i=0}^{3} J_{d,i} \bar{X}_i. \tag{26}$$

We can then substitute the resulting values of A and J into the linear relation of Eq. (18) and test this linear description of our coarse-lattice results for the 24 Cartesian data sets. The simplest test of linearity should be $\chi^2_{\mathcal{C}}$ of Eq. (20). However, for our 24 sets of seven quantities, the resulting $\chi^2_{\mathcal{C}}/(7\times 24)$ is ≈ 15 suggesting this linear description is poor. This large value of $\chi^2_{\mathcal{C}}$ comes from the linear prediction of the heavy-heavy spin-average masses. If these are dropped from the calculation of $\chi^2_{\mathcal{C}}$, we obtain $\chi^2_{\mathcal{C}}/(6\times 24) = 1.7$, a much more acceptable value. Looking more closely, we find the linear prediction for the heavy-heavy spin-average masses agrees with the calculated value with a fractional discrepancy of 1%–2% for the 24 data sets. This is certainly a reasonable accuracy given the systematic errors in determining these masses from our lattice calculation. However, since the statistical error on these quantities, which is used in our definition of $\chi^2_{\mathcal{C}}$, is of the order of 0.1%–0.2%, we should expect these large $\chi^2_{\mathcal{C}}$ values. Thus, we conclude that the linear description of the coarse-lattice results is satisfactory.

Using these results for J and A, Eq. (22) and the procedure outlined in the previous section to determine the error, we can go on to find the coarse-lattice parameters which describe the fine-lattice results:

$$\begin{aligned} X_{\mathcal{C}}^T &= \{m_0 a, c_B, c_E, \zeta\} \\ &= \{-0.018(100), 1.648(227), 0.957(904), 1.038(23)\}, \end{aligned} \tag{27}$$

where the superscript T indicates the transpose of the column vector $X_{\mathcal{C}}$. The results for $m_0 a$ and ζ are reasonably accurate. Note the relative error in $m_0 a$ should not be determined by comparing to the central value for $m_0 a$ which is shifted by the additive renormalization implied by m_{crit} to be close to zero. Rather, one should recognize that this error in $m_0 a$ corresponds to a 4% relative error in $m_{\mathrm{sa}}^{\mathrm{hh}}$. However, the errors on c_B and especially c_E are unacceptably large.

In order to better understand these large errors, we now examine the matrix $J^T \cdot J$. This matrix is closely related to the matrix $J^T W_{\mathcal{F}}^{-1} J$ which is inverted in Eq. (22) to obtain the coarse-lattice parameters. While the characteristics of the matrix $J^T W_{\mathcal{F}}^{-1} J$ are entirely similar to those of $J^T \cdot J$, we found it more natural to focus on the simpler matrix $J^T \cdot J$ whose definition does not depend on a somewhat *ad hoc* choice for the correlation matrix $W_{\mathcal{F}}$.

The eigenvalues of the matrix $J^T \cdot J$ are

$$\{9.55(15), 1.39(10), 0.000\,138(21), 0.000\,037(12)\} \tag{28}$$

with corresponding eigenvectors

$$\begin{aligned} &\{0.832(4), -0.1099(6), -0.1079(7), 0.532(6)\}, \\ &\{-0.522(7), 0.062(6), 0.085(3), 0.846(4)\} \\ &\{0.181(7), 0.81(7), 0.56(10), -0.003(6)\}, \\ &\{0.041(23), -0.57(10), 0.82(7), -0.0156(29)\} \end{aligned} \tag{29}$$

Here the eigenvectors reading top to bottom correspond to the eigenvalues in Eq. (27) reading left to right. The eigenvalues span a range of more than 5 orders of magnitude and dramatically decrease between the eigenvectors dominated by the $m_0 a$ or ζ directions and those aligned with c_B or c_E. The smallest eigenvalue corresponds to an eigenvector that has a large component in the c_E direction which leads to large error in the c_E coefficient. [Recall that

the components of the eigenvectors displayed in Eq. (28) are arranged in the order $\{m_0a, c_B, c_e, \zeta\}$.]

Given the range of quantities measured and the precision of the results, we were surprised that c_E remains to a large degree undetermined. Of course, this is precisely the result that would be obtained if we were working with a redundant set of parameters. Thus, we went back and looked carefully at the arguments which determined this set of "independent" parameters and discovered an additional field transformation that permits c_E to be transformed into c_B. This result is valid to all orders in ma and up to errors of order $(a\vec{p})^2$. This theoretical analysis is presented in the companion paper [11].

Here, we will exploit this substantial simplification and use only the three parameters m_0a, ζ, and $c_P \equiv c_B = c_E$. As is shown in the next section, within this restricted parameter space, the problem of determining m_0a, ζ, and c_P from given values for our seven measured quantities is well-posed and accurate results for these three parameters can be easily obtained making our proposed step-scaling, matching procedure quite practical.

B. Three-parameter action

We will now exploit this simplification from four action parameters to three and determine those three parameters which give coarse-lattice results agreeing with those found on the fine lattice. Specifically, we will use the action in Eq. (1) but fix $r_s = \zeta$, $r_t = 1$, and $c_E = c_B = c_P$, and study the dependence of the seven spectral quantities making up the vector Y in Eq. (19) on the three parameters m_0a, c_P, and ζ making up the vector:

$$X^{(3)} = \begin{pmatrix} m_0a \\ c_P \\ \zeta \end{pmatrix}. \tag{30}$$

As is shown in Ref. [11], a proper, mass-dependent choice for three parameters will yield on-shell quantities which are accurate to arbitrary order in $(ma)^n$ with errors no larger than $(a\vec{p})^2$.

How does this affect our analysis? We could, of course, disregard all of our four-parameter runs and collect an entirely new set of data with the restriction $c_B = c_E$. Instead we will exploit the approximate linearity of much of our four-parameter data and interpolate to obtain what we expect to be a good approximation to the results we would obtain had we chosen $c_B = c_E$.

Thus, we set $c_P = c_B$ and explicitly subtract the deviation that results from $c_E \neq c_B$ using the matrix of derivatives J determined in the four-parameter analysis above. Such an expansion in $c_B - c_E$ should be especially safe given the very weak dependence on this difference that we have seen. Hence, the coarse-lattice masses to be used in this three-parameter analysis are obtained from

$$Y_d^{(3),n} = Y_d^n + J_{d,2}(c_B^n - c_E^n). \tag{31}$$

The action parameters corresponding to each of these data sets are $X_0^{(3),n} = X_0^n$, $X_1^{(3),n} = X_1^n$, and $X_2^{(3),n} = X_3^n$. The resulting "three-parameter" data sets with $1 \leq n \leq 66$ can then be analyzed in precisely the same fashion as was done for the case of four parameters, following the steps taken in Eqs. (18)–(22).

Again we use as the center point that data set giving results closest to the results from the fine lattice, which is $(X^{(3),14})^T = \{0.0328, 1.511, 1.036\}$ from set No. 14, the Cartesian data sets 43–66, and obtain

$$(X_{\mathcal{C}}^{(3)})^T = \{m_0a, c_{\mathrm{P}}, \zeta\} = \{0.037(26), 1.50(9), 1.029(14)\}. \tag{32}$$

The errors quoted here are statistical and obtained as described in the beginning of this section by combining in quadrature the errors coming from the determination of the fine-lattice masses and the statistical uncertainties in determining the coarse-lattice parameters which reproduce those fine-lattice results.

Note that m_0a is relatively small (close to zero) as a reflection of m_{critical} for Wilson-type fermions lying close to m_{charm} for our lattice spacing. The significance of the error in m_0a can be estimated from $J_{1,1}^{(3)}$ times the error in m_0a from the average coarse data, giving a 4% effect of the error in m_0a on the resulting heavy-heavy, spin-averaged mass.

These better defined results for the case of the three-parameter action demonstrate that the singularity in the matrix that must be inverted to solve for these heavy quark parameters has disappeared. For completeness, we list the eigenvalues and eigenvectors of the 3×3 matrix $(J^{(3)})^T J^{(3)}$ to be contrasted with the singular results found for the four-parameter case in Eqs. (27) and (28):

$$\{9.77(15), 1.41(10), 0.000\,26(4)\}, \tag{33}$$

with corresponding eigenvectors,

$$\begin{aligned} &\{0.824(4), -0.2157(11), 0.524(6)\}, \\ &\{-0.504(8), 0.142(7), 0.852(4)\}, \\ &\{0.258(4), 0.9661(11), -0.008(7)\}. \end{aligned} \tag{34}$$

A comparison of Eqs. (27) and (28) with Eqs. (32) and (33) shows that the first two large eigenvalues and corresponding eigenvectors are changed very little by the reduction from four to three parameters.

Next we would like to examine the contribution to systematic error due to ignoring the quadratic terms in our analysis. Using our 24 Cartesian data sets, we can calculate both the first (J-matrix) and second derivatives (a quadratic matrix Q) directly, without using a fitting procedure. The resulting simple Taylor expansions around the center point are

$$Y_q^n = Y^{(3),14} + J^{(3)} \cdot (X^{(3),n} - X^{(3),14}) + \tfrac{1}{2}(X^{(3),n} - X^{(3),14}) \cdot Q \cdot (X^{(3),n} - X^{(3),14}), \quad (35)$$

where Q is the 3×3 tensor of second derivatives and n runs from 43 to 66 (including only the Cartesian data sets). We can now estimate how much our resulting parameters X depend on the quadratic terms and get a reasonable estimate of the systematic error.

Using this quadratic approximation, we determine the best-fit, coarse-lattice parameters $X_C^{(3)}$ by minimizing

$$\chi^2_{\mathcal{F},q} = (Y_{\mathcal{F}} - Y^{(3),14} - J^{(3)} \cdot (X_C^{(3)} - X^{(3),14}) - 1/2(X_C^{(3)} - X^{(3),14})^T \cdot Q^{(3)} \cdot (X_C^{(3)} - X^{(3),14}))^T \cdot W_{\mathcal{F}}^{-1} \cdot (Y_{\mathcal{F}} - Y^{(3),14} - J^{(3)} \cdot (X_C^{(3)} - X^{(3),14}) - 1/2(X_C^{(3)} - X^{(3),14})^T \cdot Q^{(3)} \cdot (X_C^{(3)} - X^{(3),14})). \quad (36)$$

The result is $(X_C^{(3)})^T = \{m_0 a, c_{\mathrm{P}}, \zeta\} = \{0.034(8), 1.50(3), 1.035(5)\}$, now including the effects of quadratic terms. Comparing these numbers with those in Eq. (31) from the linear approximation, one sees that the quadratic contributions to the results are buried in statistical noise. Therefore, we will not include contributions to the possible systematic errors coming from the neglect of these quadratic terms in the analysis.

The systematic errors enter as: (a) We use $(ma)^2 = 0.2^2$ or 4% as an estimate of the heavy quark discretization errors from domain wall fermion calculation on the fine lattice. (b) The remaining RHQ heavy quark discretization effects on the coarse lattice are given by $(a\vec{p})^2 = (\alpha_s(\mu = 1\ \mathrm{GeV})ma)^2 \approx 0.004$. (c) Finally we estimate 1.3% as the systematic error arising from the matching of the spatial volumes of fine and coarse lattices. Therefore, adding these three systematic errors in quadrature gives our final coefficients: $(X_C^{(3)})^T = \{m_0 a, c_{\mathrm{P}}, \zeta\} = \{0.037(26) \times (13), 1.50(9)(6), 1.029(14)(40)\}$ where the first error shown is statistical and the second systematic.

In our analysis, we have determined three parameters in the action by requiring that seven physical quantities agree between the coarse and fine lattices. Can we match fewer physical quantities between the coarse and fine-lattice spacing calculations and obtain the same result? Table X summarizes the results for various choices of the quantities being matched. As we can see, all the different choices give consistent values for our three action parameters, agreeing within one σ. Thus, we have very consistent results for different choices of calculated quantities which provides a numerical demonstration of the validity of the heavy quark version of the Symanzik improvement program being implemented here.

Let us focus on two choices of measurements: index "E" using all seven measurements and index "B" using only the results from heavy-heavy data. One might hope that the more measurements we include in the analysis, the smaller the resulting errors will be. However, it should be recognized that the cost in computer time of making the additional measurements involving light quarks is high. As we can see, despite its considerable added cost, the index E set makes only a small improvement on the statistical errors. It may be more sensible to double the number of configurations and focus exclusively on the heavy-heavy system in future calculations.

V. COMPARISONS WITH OTHER APPROACHES

The description of heavy quarks explored in this paper is one of a number of formulations built on Wilson's original fermion action [44] with the addition of clover and/or anisotropic terms. In this section we compare the parameters $m_0 a$, ζ, and c_P determined here for our $1/a = 3.6$ GeV effective heavy quark theory with similar parameters determined by two of these other methods: standard, $O(4)$-symmetric, clover-improved Wilson fermions, and the 4-parameter, anisotropic Fermilab action. This serves both as an approximate check of the results determined here and an opportunity to compare perturbative and nonperturbative methods.

A. $O(a)$-improved Wilson fermions

Since the asymmetry parameter ζ was found to be close to unity, it is of interest to compare our parameters $m_0 a$ and c_P with the corresponding mass $(m_{W0} a)$ and Sheikholeslami-Wohlert (c_{SW}) parameters which appear

TABLE X. The resulting coarse-lattice parameters obtained by matching various combinations of physical quantities between the coarse and fine lattices. Different choices of the quantities to be matched give action parameters consistent with each other within one σ, showing the consistency of this heavy quark improvement program.

Measurement index	Data used	$X_C^{(3)}$
A	$m_{\mathrm{sa}}^{\mathrm{hh}}$, $m_{\mathrm{hs}}^{\mathrm{hh}}$, $m_{\mathrm{sos}}^{\mathrm{hh}}$, m_1/m_2	{0.07(4), 1.67(13), 1.030(14)}
B	"A" + $m_{\mathrm{soa}}^{\mathrm{hh}}$	{0.04(3), 1.56(10), 1.034(12)}
C	$m_{\mathrm{sa}}^{\mathrm{hh}}$, $m_{\mathrm{hs}}^{\mathrm{hh}}$, $m_{\mathrm{sa}}^{\mathrm{hl}}$, $m_{\mathrm{hs}}^{\mathrm{hl}}$, m_1/m_2	{0.06(4), 1.62(13), 1.032(14)}
D	"D" + $m_{\mathrm{sos}}^{\mathrm{hh}}$	{0.04(3), 1.56(10), 1.034(12)}
E	All	{0.03(3), 1.53(10), 1.035(12)}

in the standard, relativistic, $O(a)$-improved, Wilson fermion action.

We first consider the Sheikholeslami-Wohlert or clover coefficient $c_{\rm SW}$. This can be obtained from the nonperturbative result of Ref. [45]:

$$c_{\rm SW} = \frac{1 - 0.656g^2 - 0.152g^4 - 0.054g^6}{1 - 0.922g^2}, \qquad (37)$$

where g is the lattice coupling constant and $\beta = 6/g^2$. This gives $c_{\rm SW} = 1.544$ for our choice of $\beta = 6.351$ which compares well with our result $c_P = 1.50(9)(6)$.

Next examine the bare Wilson mass $m_{W0}a$. For the standard, $O(a)$-improved Wilson action, this is usually related to the continuum, "physical" quark mass by a combination of a shift coming from the intrinsic chiral symmetry breaking of Wilson fermions and a multiplicative renormalization factor Z_m:

$$m(\mu) = Z_m(m_{W0} - m_{\rm crit}/a), \qquad (38)$$

where $m_{\rm crit}/a$ locates the value of m_{W0} at which the pion mass vanishes and $m(\mu)$ represents the continuum quark mass, defined by a renormalization condition imposed at the energy scale μ. In the discussion below we will use the $\overline{\rm MS}$ scheme and $\mu = 2.0$ GeV. We have introduced an explicit factor of the inverse lattice spacing in Eq. (37) to give the continuum quark mass its proper units.

We first determine the value of $m^{\overline{\rm MS}}(\mu)$ which corresponds to the $m_f = 0.2$ input mass used in our reference, $\beta = 6.638$ domain wall fermion calculation. For domain wall fermions Eq. (37) also applies but m_0 should be replaced by m_f/a and $-m_{\rm crit}$ by $m_{\rm res}$, a measure of residual domain wall fermion chiral symmetry breaking that is sufficiently small that it will be neglected here. While a quenched, $\beta = 6.638$, domain wall fermion value for Z_m is not known, the value $Z_m \approx 1.59$ obtained at $\beta = 6.0$ [22] may not be too far off. (The results presented in Ref [46] can be used to compare Z_m evaluated with the DBW2 action at two very different lattice spacings, $1/a = 1.3$ GeV and $1/a = 2.0$ where a change of less than 3% is seen.) Thus, we conclude that the calculations described in this paper correspond to $m^{\overline{\rm MS}}(\mu = 2.0\ {\rm GeV}) = 1.72$ GeV. (This large value suggests that our choice for m_f on the fine lattice may be somewhat larger than is appropriate for the charm-quark mass.)

To relate this result for $m(\mu)^{\overline{\rm MS}}$ to the value of m_{W0} expected in a physically equivalent, $O(a)$-improved Wilson calculation at $\beta = 6.351$, we next determine $m_{\rm crit}$. The critical quark mass can be estimated using either perturbative or nonperturbative methods. The two-loop, perturbative value for $m_{\rm crit}$ for the Wilson gauge and $O(a)$-improved fermion action has been obtained in Ref. [39]:

$$m_{\rm crit} = g^2\Sigma^{(1)} + g^4\Sigma^{(2)} \qquad (39)$$

$$\Sigma^{(1)} = \frac{N_c^2 - 1}{N_c}(-0.162\,857\,1 + 0.043\,483\,03c_{\rm SW} + 0.018\,095\,8c_{\rm SW}^2) \qquad (40)$$

$$\Sigma^{(2)} = (N_c^2 - 1)\Bigg[\left(-0.017\,537 + \frac{1}{N_c^2}0.016\,567 + \frac{N_f}{N_c}0.001\,186\,18\right) + \left(0.002\,601 - \frac{1}{N_c^2}0.000\,559\,7 - \frac{N_f}{N_c}0.000\,545\,9\right)c_{\rm SW} + \left(-0.000\,155\,6 + \frac{1}{N_c^2}0.002\,622\,6 + \frac{N_f}{N_c}0.001\,365\,2\right)c_{\rm SW}^2 + \left(-0.000\,163\,15 + \frac{1}{N_c^2}0.000\,158\,03 - \frac{N_f}{N_c}0.000\,692\,25\right)c_{\rm SW}^3 + \left(-0.000\,017\,219 + \frac{1}{N_c^2}0.000\,042\,829 - \frac{N_f}{N_c}0.000\,198\,100\right)c_{\rm SW}^4\Bigg], \qquad (41)$$

where the number of fermion flavors $N_f = 0$ in the quenched approximation, the number of colors $N_c = 3$, and we use the value of $c_{\rm SW} = 1.544$ determined above. This gives $m_{\rm crit} = -0.219$ for $\beta = 6.351$.

An alternative way to compute $m_{\rm crit}$ is to take the nonperturbative, ALPHA collaboration measurement of $\kappa_{\rm crit}$ (for example from Table 1 in Ref. [45]) and parametrize it as a function of coupling constant:

$$\kappa_{\rm crit} = \frac{0.130\,287 - 0.239\,546g^2 + 0.111\,829g^4}{1 - 1.849\,15g^2 + 0.868\,181g^4} \qquad (42)$$

for $6.0 \le \beta \le 7.4$ and use $m_{\rm crit} = \frac{1}{2\kappa_{\rm crit}} - 4$. This gives $m_{\rm crit} = -0.317$. We will adopt this latter, nonperturbative value as being more accurate.

Finally, in order to invert Eq. (37) to obtain the expected value of $m_{W0}a$ which can be compared with our result for m_0a, we require the appropriate factor Z_m for our rather fine $\beta = 6.351$ lattice. However, for this comparison we can avoid the extra translation to and from the $\overline{\rm MS}$ scheme by directly comparing quantities calculated in the RI scheme at $\mu = 2.0$ GeV. From Tables I and II of Ref. [22] we determine $Z_m^{\rm RI}({\rm DWF}) = 1.81$. We will use a similar nonperturbative value $Z_m^{\rm RI}({\rm SW}) = 1/Z_S^{\rm NPM} = 1.82$ extracted from Table 1 of Ref. [47]. This value is only approximate for our situation since it was obtained on a coarser, $\beta = 6.2$ lattice. Using these values we obtain $m_{W0} = Z_m^{\rm RI}({\rm DWF})/Z_m^{\rm RI}({\rm SW})\, m_f + m_{\rm crit}/a = -0.018/a$ in units of $1/a = 3.6$ GeV. Thus, we can compare our RHQ

action parameters $\{m_0a, \zeta, c_P\} = \{0.037(26)(13), 1.50(9) \times (6), 1.029(14)(40)\}$ with those for a corresponding $O(a)$-improved Wilson theory describing the same system: $\{-0.018, 1.544, 1\}$. Since the two values for m_0a should be viewed as quite close to zero, these two actions are very similar suggesting that, for a $1/a = 3.6$ GeV lattice a standard $O(a)$-improved Wilson action, with $c_{\rm SW}$ and $Z_m^{\rm RI}$ determined nonperturbatively but at zero quark mass, may describe a charmed quark at least to the accuracy of this somewhat rough comparison.

B. Four-parameter Fermilab action with one-loop coefficients

We now compare our nonperturbative result for the remaining parameters ζ and c_P with the one-loop perturbative calculations carried out by Nobes [28] for the closely related quantities, ζ, c_B, and c_E appearing in the Fermilab action.

These one-loop coefficients of Fermilab action were calculated using automated perturbation theory techniques from the scattering of a quark off of a background chromomagnetic(electric) field [28]. The calculations are done on the lattice and in the continuum and the comparison used to determine the lattice parameters.

The analytic tree-level coefficients (after being translated into our notation for the action) are

$$\begin{aligned}
\zeta^{[0]} &= \sqrt{\left(\frac{m_0a(2+m_0a)}{4(1+m_0a)}\right)^2 + \frac{m_0a(2+m_0a)}{2\ln(1+m_0a)}} \\
&\quad - \frac{m_0a(2+m_0a)}{4(1+m_0a)} \\
c_B^{[0]} &= \zeta^{[0]} \\
c_E^{[0]} &= \zeta^{[0]}\left(\frac{(\zeta^{[0]})^2 - 1}{m_0a(2+m_0a)} + \frac{\zeta^{[0]}}{(1+m_0a)}\right. \\
&\quad \left. + \frac{m_0a(2+m_0a)}{4(1+m_0a)^2}\right).
\end{aligned} \tag{43}$$

Next, the one-loop result for $\zeta^{[1]}$ is given by the formula

$$\zeta^{[1]} = -(1 + g_0^2 Z_{M_2}^{[1]}) \frac{(\zeta^{[0]})^2 + \zeta^{[0]} \sinh(\ln(1+m_0a))}{\zeta^{[0]} + \sinh(\ln(1+m_0a))}. \tag{44}$$

We use this formula and the numerical one-loop results from Tables 6.1 and 6.2 in Ref. [28] and perform an error-weighted fit to the three functions of interest, $\zeta(m_0a)$, $c_B(m_0a)$, and $c_E(m_0a)$ with expressions of the form

$$X^{[1]} = \frac{\sum_{i=0}^{3} a_i (m_0a)^i}{1 + \sum_{i=1}^{3} d_i (m_0a)^i}, \tag{45}$$

where X represents c_B, c_E, and ζ while the a's and d's are listed in Table XI. This fit implies that at $m_0a = 0.036$, the coefficients are $c_B = 1.261$, $c_E = 1.246$, and $\zeta = 1.003$, $\approx 1.4\sigma$ lower than our nonperturbatively determined coefficients: $(X_{\mathcal{C}}^{(3)})^T = \{0.037(26)(13), 1.50(9) \times (6), 1.029(14)(40)\}$. (Since the results of Nobes have $c_B \approx c_E$ we can directly compare the coefficients in his 4-parameter and our 3-parameter lattice action.)

To see directly the effects of the differences between these perturbative and nonperturbative coefficients, we should compare the resulting spectra. Although we did not use these one-loop numbers in a spectrum calculation, we can use our linear description of the dependence of the spectra on the action parameters [the coefficients J and A of Eq. (18)] to get a good idea of what the resulting masses would be were we to use these one-loop coefficients. We summarize the results in Table XII. These are reasonably close to our nonperturbative results with the largest discrepancy being the two hyperfine splittings which are 25% smaller when determined from the one-loop coefficients.

There is a second, extensive perturbative calculation of the one-loop, tadpole improved RHQ lattice action by the Tsukuba group [13]. However, because the Tsukuba action uses five parameters with $r_s \neq \zeta$, we cannot make a direct comparison. While continuum field transformations can be employed on the continuum effective Lagrangian to prove that these 5-parameter and 3-parameter descriptions should

TABLE XI. Parametrization of the one-loop coefficients of the Fermilab action using Eq. (44).

	a_0	a_1	a_2	a_3	d_1	d_2	d_3
$\zeta^{[1]}$	0.000 299 23	0.001 249 77	0.163 759	0.025 828 7	5.102 43	1.657 13	0.006 332 12
$c_E^{[1]}$	0.270 419	0.431 474	0.162 718	0.002 124 38	1.874 36	0.319 194	0.006 191 83
$c_B^{[1]}$	0.271 519	0.012 232 2	−0.000 039 117	0	0.056 595 5	0	0

TABLE XII. The expected coarse-lattice results for various choices of coefficients, $X_{\mathcal{C}}$, in the heavy quark effective action. Here the linear approximation of Eq. (18), with coefficients A and J determined from data sets Nos. 43–66, is being used to predict the corresponding physical masses.

Parameter	$m_{\rm sa}^{\rm hh}$	$m_{\rm hs}^{\rm hh}$	$m_{\rm sa}^{\rm hl}$	$m_{\rm hs}^{\rm hl}$	$m_{\rm sos}^{\rm hh}$	$m_{\rm soa}^{\rm hh}$	m_1/m_2
$X_{\mathcal{C}}^{(3)}$	1.0854(16)	0.0165(5)	0.716(4)	0.0239(16)	0.019(4)	1.206(13)	1.000(20)
$X_{\mathcal{C}}^{\rm Fermilab}$	1.1700(15)	0.0124(4)	0.763(4)	0.0194(13)	0.014(4)	1.292(13)	0.943(16)
Scaled $Y_{\mathcal{F}}$	1.0881(16)	0.0175(6)	0.725(3)	0.0267(13)	0.017(3)	1.211(8)	1.002(23)

lead to the same continuum physics up to discrepancies of order $(\vec{p}a)^2$, these transformations are not defined for the lattice variables and cannot be used to relate the one-loop coefficients of the Tsukuba action given in Ref. [13] and those determined here.

VI. SUMMARY AND OUTLOOK

In this work, we have demonstrated that it is practical to determine the coefficients of the relativistic heavy quark action nonperturbatively through a finite-volume, step-scaling technique. This has been done by matching various heavy-heavy and heavy-light mass spectrum calculations on two quenched lattices. The domain wall fermion action is used on fine lattice, where ma is relatively small, while for the coarse lattice an improved relativistic heavy quark action is used. By comparing the finite-volume predictions of these two theories, we can then determine the coefficients of the heavy quark action. In order to simplify the analysis, we assumed a linear relation between the parameters appearing in the heavy quark action and the resulting mass spectrum. (Of course, this assumption can be made arbitrarily accurate by working in a region sufficiently close to the desired solution.) The coefficients in this linear relation were determined by computing the coarse-lattice mass spectrum for a number of choices for the RHQ action. We could then use this linear relation to precisely determine those heavy quark parameters which would yield the masses implied by the fine-lattice calculations.

We initially applied this matching technique to the four-parameter version of the heavy quark action originally proposed in Ref. [8]. However, for this case, the system of linear equations that must be solved was singular within statistical errors and the resulting parameters, especially the coefficients c_B and c_E very poorly determined. This lead us to search for possible redundancy in the four-parameter action and recognize, as is discussed in detail in a companion paper [11], that a further field transformation was available that could be used to set $c_E = c_B$, reducing the number of independent parameters to three. With this restriction the problem of determining the relativistic heavy quark action is well posed and the coefficients can be accurately determined. Our result for the bare mass, clover term, and asymmetry between the space and time derivatives is $\{m_0 a, c_P, \zeta\} = \{0.037(26) \times (13), 1.50(9)(6), 1.029(14)(40)\}$, where the first error is statistical and the second systematic, excluding those coming from the quenched approximation. Finally, we included a quadratic term in the dependence of our measured masses on the action parameters and obtained a result consistent with the linear expansion.

While the calculation presented here describes the result of a single step-scaling, from $1/a = 5.4$ to $1/a = 3.6$, this procedure is robust and can be repeated leading to an accurate description of the charm-quark system on lattices of $1/a = 2.4$ and 1.6 GeV with controlled $O(a|\vec{p}|)^2$ errors [27]. We can easily decrease the statistical error by increasing the number of configurations (here 100 were used) and reduce the systematic error by starting with a finer lattice for the domain wall fermion calculation. Our use of the quenched calculation is intended to provide a computationally inexpensive study of the matching procedure.

The next step is a determination of the coefficients in this relativistic heavy quark action, appropriate for charm physics in full QCD. As discussed in Sec II, we can perform the same finite-volume, step-scaling procedure on $2 + 1$ flavor dynamical lattices. Since the long- and short-distance physics can be treated separately, we can substantially reduce the computational cost of such full QCD step-scaling by using heavier light quark sea masses in the earlier stage of matching, as long as $m_{\text{sea}}/\Lambda_{\text{QCD}}$ are equal for each pair of systems being matched. Such a calculation should be practical on presently available computers.

ACKNOWLEDGMENTS

The authors would like to thank Peter Boyle, Paul Mackenzie, Sinya Aoki, and Yoshinobu Kuramashi for helpful discussions, Taku Izubuchi and Koichi Hashimoto for their static quark potential code, Tanmoy Bhattacharya for discussion of a similar, on-shell, finite-volume approach which he had considered earlier, and members of the RBC collaboration for their help throughout the course of this work. We are also indebted to this paper's referee for suggesting a number of valuable improvements, clarifying our the presentation. In addition, we thank Peter Boyle, Dong Chen, Mike Clark, Saul Cohen, Calin Cristian, Zhihua Dong, Alan Gara, Andrew Jackson, Balint Joo, Chulwoo Jung, Richard Kenway, Changhoan Kim, Ludmila Levkova, Xiaodong Liao, Guofeng Liu, Robert Mawhinney, Shigemi Ohta, Konstantin Petrov, Tilo Wettig, and Azusa Yamaguchi for developing with us the QCDOC machine and its software. This development and the resulting computer equipment used in this calculation were funded by the U.S. DOE Grant No. DE-FG02-92ER40699, PPARC JIF Grant No. PPA/J/S/1998/00756, and by RIKEN. This work was supported by DOE Grant No. DE-FG02-92ER40699 and we thank RIKEN, Brookhaven National Laboratory, and the U.S. Department of Energy for providing the facilities essential for the completion of this work.

[1] S. M. Ryan, Nucl. Phys. B, Proc. Suppl. **106**, 86 (2002).
[2] N. Yamada, Nucl. Phys. B, Proc. Suppl. **119**, 93 (2003).
[3] A. S. Kronfeld, Nucl. Phys. B, Proc. Suppl. **129**, 46 (2004).
[4] M. Wingate, Nucl. Phys. B, Proc. Suppl. **140**, 68 (2005).
[5] M. Okamoto, Proc. Sci., LAT2005 (2006) 013 [arXiv:hep-lat/0510113].
[6] E. Eichten and B. R. Hill, Phys. Lett. B **234**, 511 (1990).
[7] B. A. Thacker and G. P. Lepage, Phys. Rev. D **43**, 196 (1991).
[8] A. X. El-Khadra, A. S. Kronfeld, and P. B. Mackenzie, Phys. Rev. D **55**, 3933 (1997).
[9] S. Aoki, Y. Kuramashi, and S.-i. Tominaga, Prog. Theor. Phys. **109**, 383 (2003).
[10] B. Sheikholeslami and R. Wohlert, Nucl. Phys. **B259**, 572 (1985).
[11] N. H. Christ, M. Li, and H.-W. Lin, Phys. Rev. D **76**, 074505 (2007).
[12] K. Symanzik, Nucl. Phys. **B226**, 187 (1983).
[13] S. Aoki, Y. Kayaba, and Y. Kuramashi, Nucl. Phys. **B697**, 271 (2004).
[14] M. Nobes and H. Trottier, Proc. Sci., LAT2005 (2005) 209 [arXiv:hep-lat/0509128].
[15] M. Luscher, P. Weisz, and U. Wolff, Nucl. Phys. **B359**, 221 (1991).
[16] M. Luscher, R. Sommer, P. Weisz, and U. Wolff, Nucl. Phys. **B413**, 481 (1994).
[17] J. Heitger and R. Sommer (ALPHA Collaboration), J. High Energy Phys. 02 (2004) 022.
[18] K. Symanzik, Nucl. Phys. **B190**, 1 (1981).
[19] M. Luscher, Nucl. Phys. **B254**, 52 (1985).
[20] M. Luscher, R. Narayanan, P. Weisz, and U. Wolff, Nucl. Phys. **B384**, 168 (1992).
[21] G. Martinelli, C. Pittori, C. T. Sachrajda, M. Testa, and A. Vladikas, Nucl. Phys. **B445**, 81 (1995).
[22] T. Blum *et al.*, Phys. Rev. D **66**, 014504 (2002).
[23] T. Blum *et al.* (RBC Collaboration), Phys. Rev. D **68**, 114506 (2003).
[24] H.-W. Lin, Nucl. Phys. B, Proc. Suppl. **140**, 482 (2005).
[25] H.-W. Lin, Phys. Rev. D **73**, 094511 (2006).
[26] H.-W. Lin and N. H. Christ, Proc. Sci., LAT2005 (2006) 225 [arXiv:hep-lat/0510111].
[27] H.-W. Lin, Proc. Sci., LAT2006 (2006) 184.
[28] M. Nobes, publication number: AAT NR03173 (2004).
[29] H.-W. Lin, Nucl. Phys. B, Proc. Suppl. **129**, 429 (2004).
[30] M. Guagnelli, R. Sommer, and H. Wittig (ALPHA Collaboration), Nucl. Phys. **B535**, 389 (1998).
[31] S. Necco and R. Sommer, Nucl. Phys. **B622**, 328 (2002).
[32] M. Creutz, Phys. Rev. D **21**, 2308 (1980).
[33] N. Cabibbo and E. Marinari, Phys. Lett. **119B**, 387 (1982).
[34] R. Sommer, Nucl. Phys. **B411**, 839 (1994).
[35] M. Albanese *et al.* (APE Collaboration), Phys. Lett. B **192**, 163 (1987).
[36] K. Hashimoto and T. Izubuchi (RBC Collaboration), Nucl. Phys. B, Proc. Suppl. **140**, 341 (2005).
[37] Y. Aoki *et al.*, Phys. Rev. D **72**, 114505 (2005).
[38] E. Follana and H. Panagopoulos, Phys. Rev. D **63**, 017501 (2000).
[39] H. Panagopoulos and Y. Proestos, Phys. Rev. D **65**, 014511 (2001).
[40] Y. Aoki *et al.*, Phys. Rev. D **69**, 074504 (2004).
[41] N. H. Christ and G. Liu, Nucl. Phys. B, Proc. Suppl. **129**, 272 (2004).
[42] G.-f. Liu, Report No. uMI-31-04827.
[43] P. Boyle (UKQCD Collaboration), J. Comput. Phys. **179**, 349 (2002).
[44] K. G. Wilson, in *Proceedings of the First Half of the 1975 International School of Subnuclear Physics, Erice, Sicily, 1975*, edited by A. Zichichi (Plenum Press, New York, 1977), p. 69.
[45] M. Luscher, S. Sint, R. Sommer, and H. Wittig, Nucl. Phys. **B491**, 344 (1997).
[46] C. Dawson (RBC Collaboration), Nucl. Phys. B, Proc. Suppl. **119**, 314 (2003).
[47] D. Becirevic *et al.*, Phys. Lett. B **444**, 401 (1998).